INVESTIGATIONS OF SURFACES AND INTERFACES USING OPTICAL
EXCITATION OF SURFACE PLASMONS

FINAL Technical Report

by

F. ABELES
T. LOPEZ-RIOS

January 1978
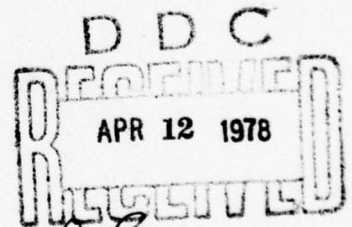
Laboratoire d'Optique des Solides, Université P. et M. Curie,
Paris, France.

R&D 2103

REPORT DOCUMENTATION PAGE

READ INSTRUCTIONS
BEFORE COMPLETING FORM

1. REPORT NUMBER	2. GOVT ACCESSION NO.	3. RECIPIENT'S CATALOG NUMBER

4. TITLE (and Subtitle)

Investigations of Surfaces and Interfaces Using Optical Excitation of Surface Plasmons.

5. TYPE OF REPORT & PERIOD COVERED

Annual Technical Report.
May 1976 - Jan 1978

6. PERFORMING ORG. REPORT NUMBER

7. AUTHOR(s)

F. Abeles
T. Lopez-Rios

8. CONTRACT OR GRANT NUMBER(s)

DAERO-75-G-027

9. PERFORMING ORGANIZATION NAME AND ADDRESS

Laboratoire d'Optique des Solides
Universite P et M Curie
Paris, France

10. PROGRAM ELEMENT, PROJECT, TASK AREA & WORK UNIT NUMBERS

6.11.02A-1T161102B11B-00-491

11. CONTROLLING OFFICE NAME AND ADDRESS

US Army Research & Standardization
Grp (Europe) Box 65, FPO NY 09510

12. REPORT DATE

Jan 1978

13. NUMBER OF PAGES

85

14. MONITORING AGENCY NAME & ADDRESS(if different from Controlling Office)

15. SECURITY CLASS. (of this report)

Unclassified

15a. DECLASSIFICATION/DOWNGRADING SCHEDULE

16. DISTRIBUTION STATEMENT (of this Report)

Approved for Public Release
Distribution Unlimited

17. DISTRIBUTION STATEMENT (of the abstract entered in Block 20, if different from Report)

18. SUPPLEMENTARY NOTES

19. KEY WORDS (Continue on reverse side if necessary and identify by block number)

Surface Plasmons: Metal Surfaces: Electrode Surfaces:
Attenuated Total Reflectance: Ellipsometry:

20. ABSTRACT (Continue on reverse side if necessary and identify by block number)

SEE OVER

406 163

A method for the study of surfaces and interfaces based on the optical excitation of surface plasmons by the attenuated total reflection method is presented. The metallic adsorption of Ag, Au on Ag, Au and Al substrates under ultra high vacuum are studied. The $Au/H_2SO_4 1N$ and $Au/HC1O_4 1N$ interfaces are also considered.

INVESTIGATIONS OF SURFACES AND INTERFACES USING OPTICAL EXCITATION OF SURFACE PLASMONS

Abstract

A method for the study of surfaces and interfaces based on the optical excitation of surface plasmons by the attenuated total reflection method is presented. The metallic adsorption of Ag, Au on Ag, Au and Al substrates under ultra high vacuum are studied. The Au/H_2SO_4 1N and $Au/HClO_4$ 1N interfaces are also considered.

In this final report we summarize the results obtained under
this grant on the investigation of surfaces and interfaces using
optical excitation of surface plasmons. The aim of this work was
to suggest and test improvements in the optical methods for the
study of metallic surfaces. Optical techniques were not widely
employed in the past in surface studies due to their lack of
surface sensitivity, which is related to the great penetration
depth of light compared to atomic distances. In spite of these
difficulties, many successful improvements were attained in
experiments conducted with light, mainly in two ways:

a) by a sophistication of the experimental techniques leading
to improved sensitivity and accuracy, like high resolution
ellipsometry with fast automatic ellipsometer and differential
measurements;

b) by the search for situations in which the light wave becomes
more surface sensitive, for instance by using resonant cavities
(1), (2) or by the excitation of surface polaritons (SPW) to
which we have dedicated ourselves.

Experiments enable now the detection and accurate characterization
of extremely small modifications of the surface, like absorption
in the monolayer range or modifications of the electronic charge
at the surface (see Appendix VI). From the theoretical point of
view, the situation is much more difficult and a non-local
theory should be employed in order to interpret most of the
experimental results, such as:

a) the reflectivity at a clean metallic surface, taking really
into account the effects produced there. Very recently the
effect of electronic inhomogeneities on the reflectivity was
studied for free electron metals (3), (4);

b) the adsorption of ad-atoms and very thin layers where macroscopic models cannot be employed. In all the work presented here, where we studied anodic oxidation and metallic adsorption, we have used the simple model of a thin film characterized by a thickness and a complex dielectric constant, and we have shown that such an approximation is quite satisfactory in most cases.

In this report, we shall present the advantages of SPW spectroscopy and illustrate them by a few examples taken from our work performed under this grant. We shall then briefly describe the results which we have obtained in two distinct areas: investigation of metallic adsorption on a metal surface, and of metal/electrolyte interfaces. Various publications giving and discussing at length these results are joined to this report as Appendices and should be consulted for additional information.

Surface plasma waves spectroscopy

A very sensitive situation is reached by coupling photons to the surfaces, that is to say by exciting surface plasma waves (SPW). In the infrared, these waves can propagate over macroscopic distances and the technique of two coupled prisms can be employed to explore metallic surfaces (5). SPW are excited in our case by an ATR (attenuated total reflection) method in the Kretschmann configuration (prism - metallic layer - transparent material).

SPW are interesting in two ways:
1) a very high surface sensitivity: the electromagnetic field is localized and amplified at the surface in a resonant manner. Fig. 1 shows the variation of the ellipsometric parameters Ψ and Δ during the formation and reduction of anodic gold oxide with SPW and in the usual configuration. The amplification of the Ψ and Δ variations obtained with SPW excitation is at least one order of magnitude;
2) the measurement of the reflection coefficient R_p in the

vicinity of the resonance as a function of wavelength or as a function of angle of incidence provides in a straightforward way a lot of physical information. The effects of surface modifications on the R_p resonances were carefully studied under this grant and are now well understood. In Appendix I., it is shown how the Υ and Δ resonances are related to the metallic surfaces and it is explained in detail how the Ψ and Δ variations are related to the surface modifications. Fig. 2 shows the modification of the R_p resonance at the surface of a Ag film (d = 653 Å) due to Pd layers of increasing thickness: 1.5, 3, 5 and 8 Å as determined with an oscillating quartz balance. The sensitivity of the method is clearly apparent from the various curves. The angular (or spectral) position of the minimum of the R_p curves as a function of the wavevector (or wavelength) provides the SPW dispersion relation. The width of the resonance is indicative of the propagation length or the wave-packet life-time of the SPW. All these informations were successfully used in our investigations. Fig. 3 shows, for instance, the SPW dispersion relations for a free Ag surface and for the same surface covered by thin Au layers 11.5, 28, 35 Å thick (upper curves) and for a Au surface free and then covered by Ag layers 6 and 14 Å thick (lower curves). It can be seen that Au layers bring the Ag dispersion curve closer to the Au dispersion curve and vice-versa.

In the present work, we were interested mainly in two kinds of experiments:
a) spectrophotometric investigation of metallic adsorbates on Ag, Au and Al surfaces in ultra-high vacuum;
b) ellipsometric and potentiometric investigation of the Au/ H_2SO_4, 1N and Au/H11O$_4$, 1N interfaces.

a) Metallic adsorption

The first practical idea is that, if the thickness of the superficial film d_f is known, then its dielectric constant

can be obtained accurately in most cases. In the present state
of optical technology, the only limiting problem is the validity
of the method used to interpret the experimental data, parti-
cularly the validity of the concept of dielectric constant for
such extremely thin layers. Realistic models which could be
tested in experiments are still to be built.

In the Appendix II we give the results of an investigation of
the optical constants of very thin Au surface layers on Ag by
taking R_p as a function of φ. In the Appendix III it is shown
that not only ε_f but also the thickness d_f of the surface layer
can be obtained simultaneously, by using all the information
provided by the R_p values as a function of λ and φ. It is
found that the continuous model is a good one for very thin
layers ($d_f \simeq 10$ Å), even for discontinuous films. It is also
found that, for many practical purposes very thin Au layers
behave very similarly to bulk Au. A more careful analysis shows:
- a shift of the Au absorption edge to higher energies and an
increase of the absorption intensity at the edge;
- an increase of the optical constants in the free electron
region, probably due to the reduction of the electron mean free
path which is limited by the dimensions of the microcrystals
constituting the very thin films.

A singular situation occurs when the dielectric constant of the
surface layer goes through zero. A striking effect is obtained,
namely a splitting of the SPW dispersion relation around the
plasma frequency of the surface layer. This effect is studied
in Appendix IV for a free electron metal and the SPW dispersion
relation is computed both for complex values of the frequency
and of the wavevector. It is shown that, in experiments conducted
at variable angle of incidence, the gap between the two branches
of the dispersion curve disappear for increasing damping in the
film. Appendix V provides experimental evidence for the predicted
effect in the case of Ag on Al. SPW dispersion curves are also
computed, taking into account absorption from optical transitions
between d and s-p bands in Ag in the explored spectral range.

For an Ag layer 26 Å thick, good agreement is found with computed curves. For thicker layers a discrepancy which increases with thickness is found and it is tentatively explained by roughness effects.

b) Au-electrolyte interface

One important advantage of this technique is that it is non-destructive and can be applied to interfaces as well. We have studied the Au-$HClO_4$, 1N and Au-H_2SO_4, 1N interfaces in two distinct potential ranges.

1. Double layer region

In this region, the main effect is the polarization of the interface. Different applied voltages give rise to modifications of the electrolyte double layer. In the metal, the electronic inhomogeneity extends over a few atomic layers only. In the electrolyte, the modifications occur in the first ionic layer close to the electrode surface and in the ionic diffuse layer.

In Appendix VI, we give the results of an investigation of the Au/$HClO_4$ and Au/H_2SO_4 interfaces and we show that it is possible to separate the modifications induced by the applied voltage in the electrolyte from those induced in the metal. With the very simple Aspnes-McIntyre model it was found that, for not too large applied voltages, the penetration of the d.c. electric field is about 1-1.5 times the Thomas-Fermi screening length. The electrolyte modifications are interpreted in terms of specific adsorption.

2. Au anodic oxide

The anodic oxidation of gold has been investigated, the electrolyte being a H_2SO_4, 1N solution. The charge Q entering the oxide formation has been measured by coulommetry. The optical results

display a very clear change in the ξ (oxide) vs. Q for Q = 7.50 μC/cm^2, which is probably related to the formation of a monolayer of oxide. It was impossible to determined simultaneously the dielectric constant $\mathcal{E}_{1f} - i\mathcal{E}_{2f}$ and the thickness d_f of the layer. A limitation of the range of possible values of d_f is obtained if $\mathcal{E}_{1f}$ and $\mathcal{E}_{2f}$ are kept within physically reasonable limits. The thickness of the Au oxide layer is a few ängstroms.

References

1. N.J. HARRICK, J. Opt. Soc. Am. 60 (1970), 499.

2. F. ABELES, J. of Vac. Sci. and Tech. 9 (1972), 169.

3. P.J. FEIBELMAN, Phys. Rev. B 14 (1976), 762
    and Phys. Rev. B 12 (1975), 1319.

4. AMITABHA BAGHI, Phys. Rev. B 15 (1977), 3060.

5. J. SCHOENWALD, E. BURSTEIN and J.M. ELSON, Solid. State
    Comm. 12 (1973), 185.

Figure captions

Figure 1 : Recording of the ellipsometric parameter Ψ and Δ
for changing electrode potential V in the usual
configuration and in an ATR onciguration with
excitation of SPW.

Figure 2 : R_p vs. λ for an Ag film 653 Å thick and covered by
Pd layers 1.5, 3, 5 and 8 Å thick. The external angle
of incidence was θ = 39.58.

Figure 3 : Surface plasmon dispersion curves $\lambda(\varphi)$ for bare
silver and for silver covered by Au layers 11.5, 28,
35 Å thick; also for bare Au and for Au covered by
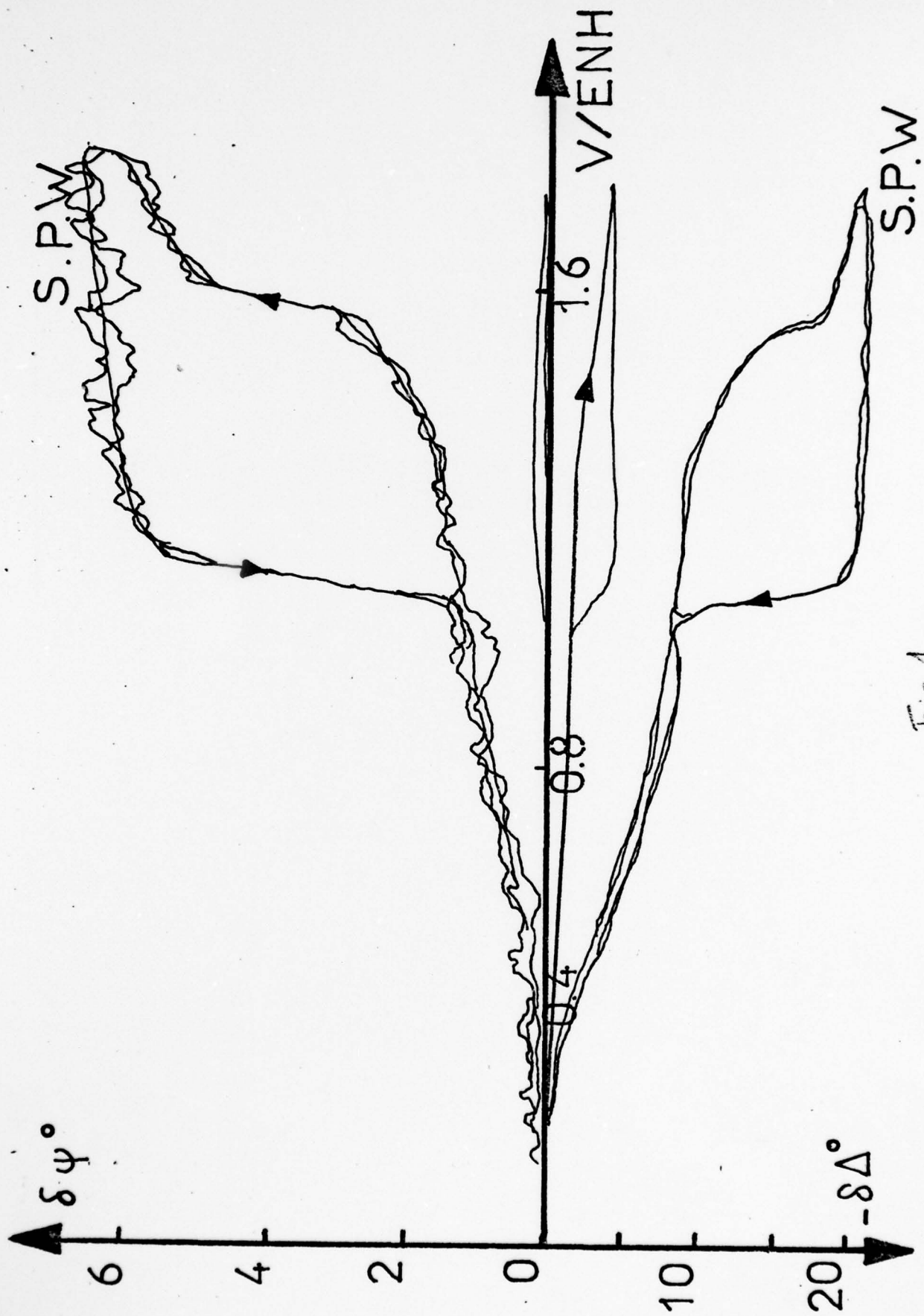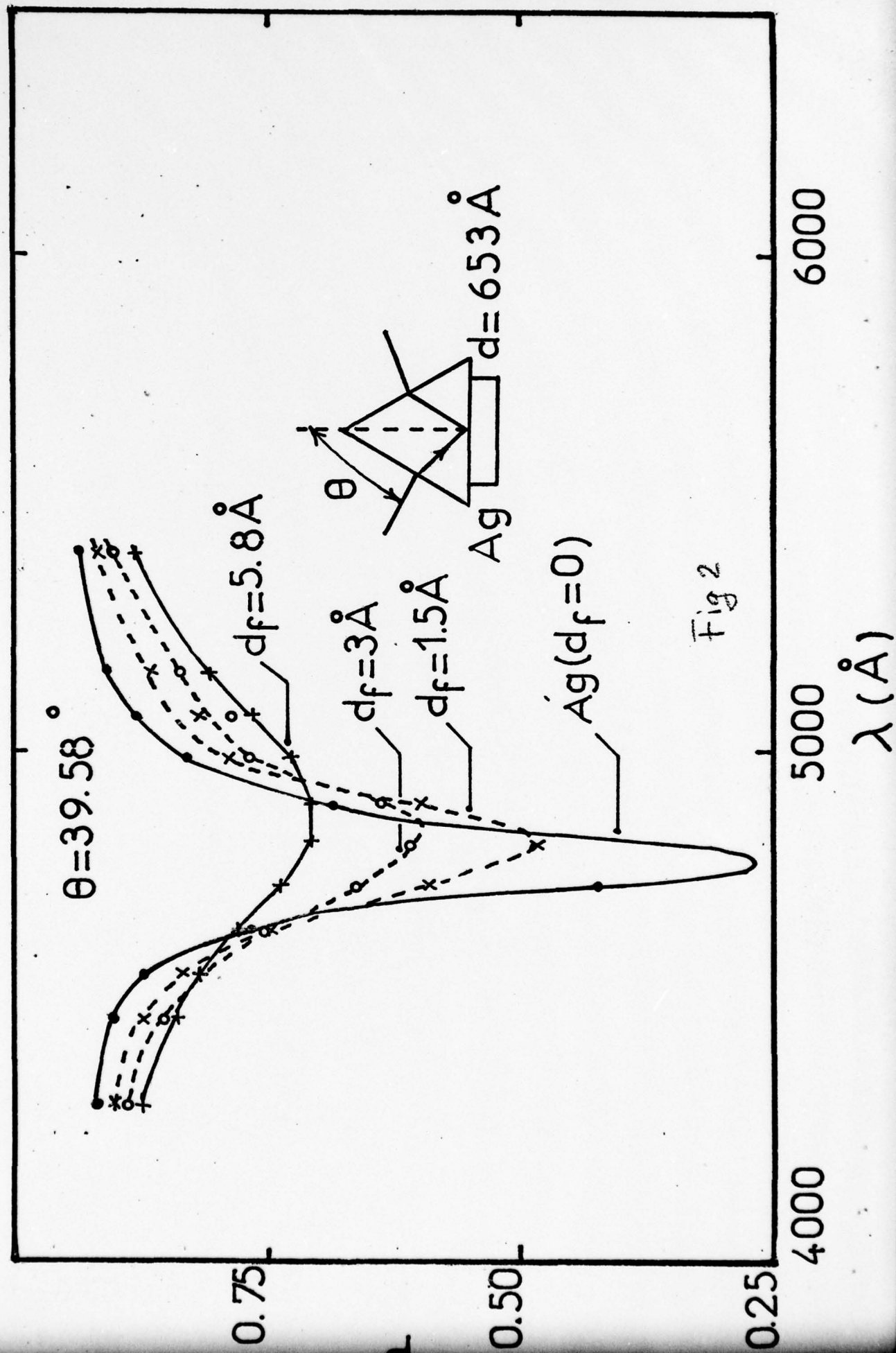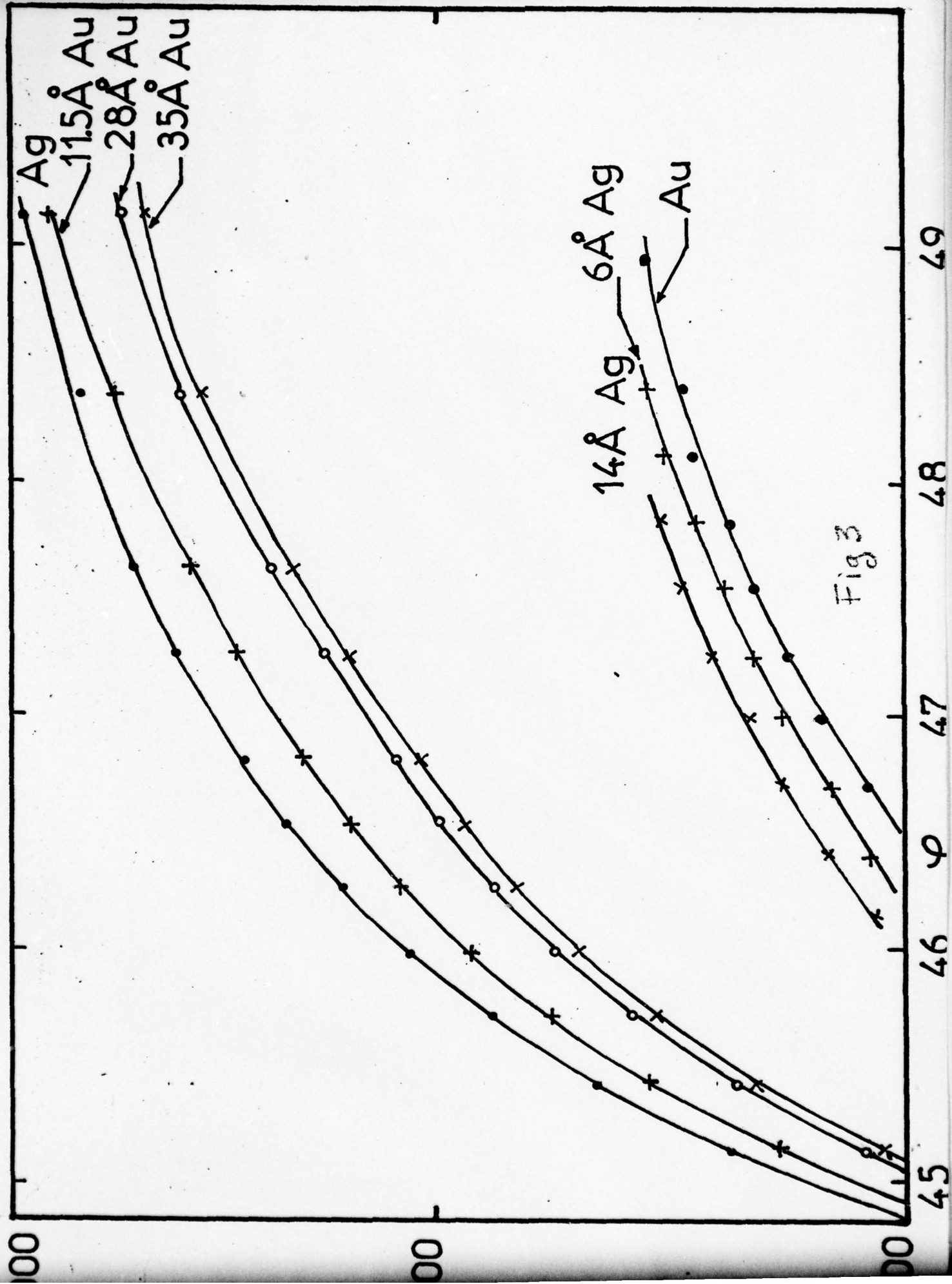Ag layers 6 and 14 Å thick.

Fig 1

Fig 2

Fig 3

APPENDIX I

SURFACE ELECTROMAGNETIC WAVES ELLIPSOMETRY

F. ABELÈS

Laboratoire d'Optique des Solides *, Université Paris VI,
4, place Jussieu, 75230 Paris Cédex 05, France

After a brief description of surface electromagnetic waves (SEW), this paper describes their optical excitation and ellipsometric detection. It is shown how tan ψ and Δ are related to the characteristic optical properties of the various media and a special description of the Δ variations as a function of k is given (k is the component of the wavevector along the surface). The possibilities offered by this technique for the investigation of surface or interface reactions are indicated.

1. Introduction

Although surface electromagnetic waves (SEW), i.e. electromagnetic waves propagating along the plane interface between two media, have been already theoretically investigated during the first decade of this century (Zenneck [1], Sommerfeld [2]), it is only during the last few years that they have attracted the interest of the experimentalists. This is due to the fact that methods have been found which enable the optical excitation and detection of SEW. The methods of generating the SEW using attenuated total reflections will be described in section 3, which follows the description of SEW given in section 2. The detection is usually performed by measuring the reflected intensity of a p-polarized incident beam. Here, we shall discuss the information gained by using the ellipsometric detection of SEW. Although, in principle, intensity measurements provide enough information, we shall see the advantages of using, besides intensity measurements, phase measurements too. The theory relating the ellipsometric response function tan ψ exp(iΔ) to the parameters characterizing the various media is given in section 4. We illustrate the various theoretical results either with experimental or with computed curves. The aim is to stress the possibilities offered by this technique for the investigation of surface or interface reactions. These are discussed in section 5. A summary and some remarks are given in the concluding section.

2. Description of SEW

SEW are plane electromagnetic (EM) waves propagating along the interface of two semi-infinite media which are evanescent in both media. If the interface is in the xy plane and if xz is the sagittal plane, containing the propagation vector and the normal to the interface, the frequency and space dependence of the field vectors in both media is $\exp[\pm\alpha z + i(\omega t - kx)]$. According to our definition, the SEW are guided surface EM waves. It can be shown that Maxwell's equations have solutions satisfying the above requirements only when one of the adjacent media has a negative dielectric constant and when k is a particular function of the dielectric constants of both media. The latter being frequency dependent, it follows that there will be a functional relation between k and ω, usually called a dispersion relation. Moreover SEW can be found only for a p-polarized EM wave. A thorough discussion and description of the SEW can be found in a few recent papers (Burstein et al. [3], Economou and Ngai [4]).

We give here the results which are obtained from the above definition and description of SEW. This enables us to indicate the notations to be used in this paper. The production or excitation of SEW will be discussed in the next section. The medium with a negative dielectric constant will be the $\epsilon = \epsilon_1 - i\epsilon_2$ medium, usually called the surface active medium. Its dielectric constant is in fact complex, but we shall assume that $\epsilon_2 \ll |\epsilon_1|$ and $\epsilon_1 < 0$, thus ϵ is essentially negative. The positive dielectric constant of the adjacent medium, usually called surface inactive, is ϵ_0 and it is usually practically constant over the frequency range of interest. In order to satisfy the boundary conditions at the $z = 0$ plane, k, the component of the wave vector along the interface, must be the same in both media. The damping coefficients α of the waves in the z direction are given by

$$\alpha^2 = (\omega/c)^2 \epsilon - k^2 , \qquad \alpha_0^2 = (\omega/c)^2 \epsilon_0 - k^2 , \tag{1}$$

both α^2 and α_0^2 being positive numbers. The dispersion relation reads:

$$k^2 = (\omega/c)^2 \epsilon\epsilon_0/(\epsilon + \epsilon_0) . \tag{2}$$

When ϵ is complex, k is complex too. This means that there is a damping of the SEW when propagating along the interface, and this is due to the fact that the surface active medium is absorbing ($\epsilon_2 > 0$). If $k = k_1 - ik_2$, and $\epsilon_2 \ll |\epsilon_1|$, then

$$k_1 = \left(\frac{\omega}{c}\right)\left(\frac{\epsilon_1\epsilon_0}{\epsilon_1 + \epsilon_0}\right)^{1/2} = \left(\frac{\omega}{c}\right)S_{m1} , \qquad k_2 = \left(\frac{\omega}{c}\right)\frac{\epsilon_2}{2\epsilon_1^2}S_{m1}^3 = \left(\frac{\omega}{c}\right)S_{m2} . \tag{3}$$

According to its definition, k must be mainly real and this imposes a more stringent condition on ϵ_1, namely $\epsilon_1 < -\epsilon_0$. Eq. (3) shows that $k_2 \ll k_1$, i.e. the SEW is only slightly damped.

The point to be noticed is that eq. (2) is a resonance condition and this explains why SEW are so sensitive to the surface conditions. Indeed, according to eq. (1), it

can be shown that the penetration depth of the EM waves in both media α^{-1} and α_0^{-1} is rather large (a few hundred angstrom units).

Eq. (2) alone is not enough in order to make sure that we are dealing with SEW. Indeed if ϵ and ϵ_0 are both real and positive, it is the condition for the nulling of the p-polarized reflected wave. For a given frequency, it defines the Brewster angle.

Combining the results obtained for homogeneous and for evanescent waves, it can be concluded that eq. (2) is the condition for having one and only one wave in each of the adjacent media.

3. Optical excitation of SEW

It is well known that the EM wave in the surface active medium ($\epsilon_1 < 0$) is a quasi-evanescent wave in all circumstances. Therefore, in order to excite a SEW two conditions must be fulfilled besides using a p-polarized wave, namely: (a) having an evanescent wave in the surface inactive medium and (b) fulfilling the condition (2). The former is realized by using a total reflection prism, i.e. a prism (or half-cylinder, or half-sphere) with dielectric constant $\epsilon_p > \epsilon_0$, and an angle of incidence ϕ_p larger than the critical angle for total reflection. The condition (2) is fulfilled either by varying ϕ_p at fixed frequency or by varying ω at fixed incidence ϕ_p. Indeed, we have $k = (\omega/c)\epsilon_p^{1/2} \sin \phi_p$ and its value can be adjusted by acting either on ω or on ϕ_p.

According to the above considerations, two configurations are possible in order to excite SEW at the ϵ/ϵ_0 interface. The first, in which the prism is in contact with the surface inactive medium, has been proposed by Otto [5] and is shown in fig. 1a. The second, in which the prism is in contact with the surface active medium, has been suggested by Kretschmann [6] and is shown in fig. 1b. The ϵ_0/ϵ interface is at a distance d from the prism and d being finite, it is obvious that the prism will modify somewhat the SEW. In fact, as we shall see below, there is an optimum value of d, say d_m, for which the sensitivity for the detection is a maximum and d_m is of the order of a fraction of the wavelength used for the detection.
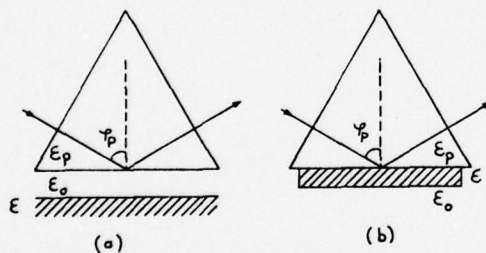

Fig. 1. Two configurations used in order to excite SEW at the ϵ/ϵ_0 interface: (a) the prism is in contact with the surface inactive medium ϵ_0, which is often air (Otto [5]); (b) the prism is in contact with the surface active medium ϵ (Kretschmann [6]).

4. Detection of SEW

We shall establish first the expression for the ellipsometric response function $\tan \psi \exp(i\Delta)$ when SEW are optically excited as described in the preceding section. Here ψ and Δ have the usual meaning, i.e.

$$\tan \psi \exp(i\Delta) = r_p/r_s ,$$

where r_p and r_s are the reflected complex amplitudes for p- and s-polarized incident waves. From the considerations concerning the value of d, it is likely that r_s will be practically constant over the investigated range of values of r_p. Moreover, in the medium which is in contact with the prism carrying evanescent or quasi-evanescent waves, $|r_s| \approx 1$. The approximate expression for $\tan \psi \exp(i\Delta)$ to be given below assumes $|r_s| = 1$, therefore the true value of $\tan \psi$ may be a few percent larger than the indicated one.

We assume that we are working at fixed frequency and variable ϕ_p, i.e. variable k. Let us call $k_m = k_{m1} - i k_{m2}$ the solution of eq. (2) as given by eq. (3). We assume first that we are working in the configuration described by fig. 1b. We define a complex quantity Δk_m, which is some respects takes into account the influence of the prism and of the finite thickness d of the surface active medium:

$$\Delta k_m = \Delta k_{m1} - i\Delta k_{m2} = \left(\frac{\omega}{c}\right) \frac{2S_{m1}^3}{-\epsilon_1 + \epsilon_0} \exp(-2\alpha d) \exp(i\delta_1) , \tag{4}$$

where α has been defined in eq. (1) and δ_1 is the phase change on reflection for a p-polarized wave at the prism/surface active film interface. It can be shown [7] that

$$\tan \psi \exp(i\Delta) \approx \exp(i\Delta_m) \frac{k - k_m - \Delta k_m^*}{k - k_m - \Delta k_m} . \tag{5}$$

Here Δk_m^* is complex conjugate to Δk_m and Δ_m, in a crude first approximation, is the value of Δ for the ϵ_p/ϵ interface. For the Otto configuration, eq. (5) is still valid, but Δk_m must be defined accordingly.

Eq. (5) is the ellipsometric response function to optically excited SEW. It represents a resonant response, as can be seen by discussing separately the variations of ψ and Δ. We have

$$\tan^2 \psi = \frac{(k - k_{m1} - \Delta k_{m1})^2 + (k_{m2} - \Delta k_{m2})^2}{(k - k_{m1} - \Delta k_{m1})^2 + (k_{m2} + \Delta k_{m2})^2} , \tag{6}$$

and

$$\tan(\Delta - \Delta_m) = \frac{2\Delta k_{m2}(k - k_{m1} - \Delta k_{m1})}{(k - k_{m1} - \Delta k_{m1})^2 + k_{m2}^2 - \Delta k_{m2}^2} . \tag{7}$$

Eq. (6) is typical of a resonance curve with a minimum for $k = k_{m1} + \Delta k_{m1}$. The minimum value of ψ is given by

$$\tan \psi_m = \left| \frac{k_{m2} - \Delta k_{m2}}{k_{m2} + \Delta k_{m2}} \right|. \tag{8}$$

We have seen that the condition for the excitation of SEW is $k = k_{m1}$ [eq. (3)]. Due to the presence of the coupling prism, this condition is slightly modified ($\Delta k_{m1} \ll k_{m1}$). According to eq. (8), $\psi_m = 0$ when $k_{m2} = \Delta k_{m2}$, i.e. when the two damping mechanisms have equal intensity. This equation can be solved to find the value of d_m discussed in section 2. When d is very large, $\Delta k_m \to 0$ and the resonance occurs at $k = k_{m1}$ but its contrast is extremely small ($\psi_m \approx 45°$) and it becomes very difficult to detect. For d smaller or larger than d_m, ψ_m can have the same value, that is to say it is impossible to say something definite from the intensity of the resonance alone. On the other hand, the halfwidth of the resonance $k_{m2} + \Delta k_{m2}$ is characteristic of d: it decreases exponentially with d.

Usually, SEW resonances are detected by measuring the reflectance R_p for a p-polarized wave in the configurations of fig. 1. As $R_p = |r_p|^2$ and as we have seen that
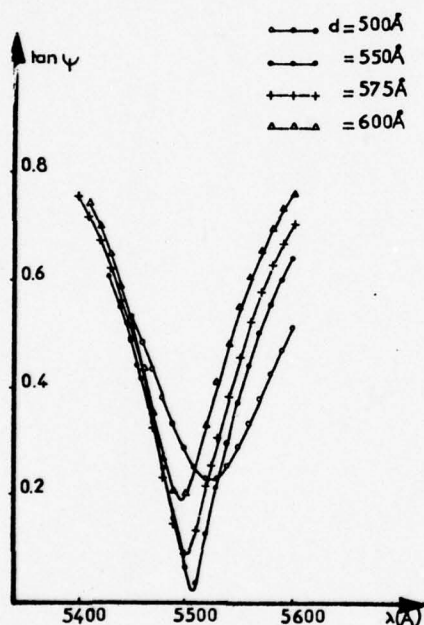

Fig. 2. Tan ψ versus λ at fixed incidence ($\phi_p = 33.3°$) for various film thicknesses ($d = 500$ to 600 A) in the configuration of fig. 1b. The dielectric constants of the various media are $\epsilon_p = (1.89)^2$, $\epsilon_0 = 1$ and $\epsilon = 4 - (\lambda/\lambda_p)^2/[1 - i(\lambda/\lambda_\tau)]$ with $\lambda_p = 1290$ A and $\lambda_\tau = 3 \times 10^5$ A.

$|r_s| \approx 1$, it follows that $\tan^2 \psi$ is practically equal to R_p. From this point of view, ellipsometry brings nothing new with respect to reflectometry.

Let us examine now the variations of Δ with k according to eq. (7). We have indicated that r_s is practically constant over the resonance region, therefore $\Delta = \arg(r_p) - \arg(r_s)$ is a measure of the variations of $\arg(r_p)$. The variations of Δ are different for $d < d_m$ and for $d > d_m$. For $d < d_m$, Δ shows an amplitude of variation which is larger than 180°. Indeed for $k = k_{m1} + \Delta k_{m1} \mp (\Delta k_{m2}^2 - k_{m2}^2)^{1/2}$ we have $\Delta = \Delta_m \pm 90°$, Δ_m being the Δ value at the resonance. On the other hand, when $d > d_m$, $k_{m2} > \Delta k_{m2}$, and reaches a maximum (Δ_{max}) and a minimum (Δ_{min}) for values of k which are close to and symmetrical with respect to the resonance. Indeed we have

$$\tan(\Delta_{max} - \Delta_m) = \tan(\Delta_m - \Delta_{min}) = \tan \tfrac{1}{2}(\Delta_{max} - \Delta_{min})$$

$$= \Delta k_{m2}(k_{m2}^2 - \Delta k_{m2}^2)^{-1/2} ,$$

when $k = k_{m1} + \Delta k_{m1} \mp (k_{m2}^2 - \Delta k_{m2}^2)^{1/2}$.

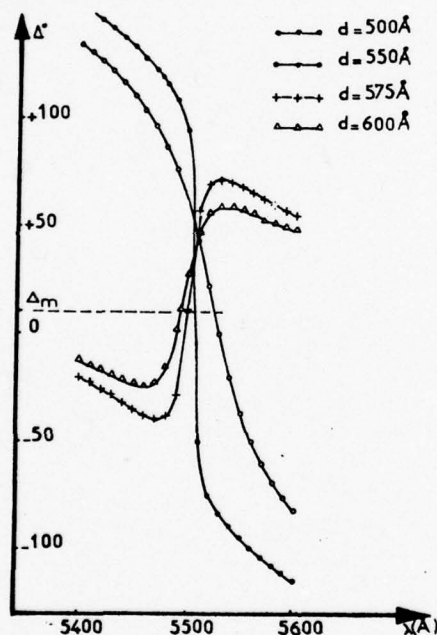From this discussion, it is immediately apparent that the value of d with respect

Fig. 3. Δ versus λ corresponding to the same configuration and data as in fig. 2. The curves corresponding to $d = 500$ and 550 A have been shifted vertically by 180° in order to draw them on the same figure. This point will become clear when comparing these curves with Δ of fig. 8.

to d_m is deduced from a mere inspection of the Δ versus k variations. As these are symmetrical with respect to $k = k_{m1} + \Delta k_{m1}$, it is apparent that Δ_m is an inflection point for the Δ versus k curve.

According to our approximate eq. (5), the SEW resonance can be described by five quantities: Δ_m, k_m and Δk_m. Four of these, namely Δ_m, $k_{m1} + \Delta k_{m1}$, k_{m2} and Δk_{m2} can be deduced immediately from an inspection of the Δ versus k curve. The use of the ψ versus k variations does not bring any new information. It is also apparent from eq. (5) that $\tan \psi$ and Δ are Kramers–Kronig transforms in k space, which is not surprizing if we remember that they are the modulus and the argument of r_p respectively.

The above considerations are illustrated by figs. 2 and 3. They correspond to the Kretschmann configuration with $\epsilon_p = (1.89)^2$ and $\epsilon_0 = 1$. The surface active medium is silver described by its dielectric constant $\epsilon = 4 - (\lambda/\lambda_p)^2/[1 - i(\lambda/\lambda_\tau)]$ with $\lambda_p = 1290$ Å and $\lambda_\tau = 3 \times 10^5$ Å. Fig. 2 shows the $\tan \psi$ versus k variations for various film thicknesses ($d = 500$ to 600 Å) and a fixed incidence $\phi_p = 33.3°$. The remarks concerning the ψ versus k curves can be verified: $d_m \simeq 550$ Å and ψ_m has almost the same value for $d = 500$ Å and 600 Å, but the halfwidth of the curves decreases with increasing thickness of the surface active film. Fig. 3 shows the Δ versus λ for the same configuration as fig. 2. Here the limiting value d_m is strikingly apparent. Indeed the curves for $d = 575$ Å and 600 Å show a maximum and a minimum, whereas those for $d = 500$ Å and 550 Å display a monotonous variation over a very large interval of Δ values. For $d = 550$ Å, which almost corresponds to d_m the variations are particularly rapid in the vicinity of $\lambda = 5510$ Å, which is the resonance wavelength. The symmetry of the curves is also apparent and we have indicated Δ_m which has practically the same value for all the thicknesses.

5. Modification of the SEW by a very thin layer

We have already indicated that the optical excitation of SEW is very sensitive to the interface characteristics. For instance, SEW are modified by the roughness of the interface. This has been verified by Braundmeier and Arakawa [8] using the measurement of R_p. The observed modifications are essentially a shift of the position of the resonance and a broadening. They can be described phenomenologically by the addition of a complex quantity $\delta k = \delta k_1 - i\delta k_2$ to the numerator and denominator of eq. (5), δk_1 being related to the shift and δk_2 to the broadening of the resonance:

$$\tan \psi \, \exp(i\Delta) = \exp(i\Delta_m) \frac{k - k_m - \delta k - \Delta k_m^*}{k - k_m - \delta k - \Delta k_m}. \tag{9}$$

These quantities are related to the r.m.s. height of the roughness and to the coherence length of the roughness in a way which has not yet been completely indicated, although they could be deduced from a first order theory such as the one elaborated by Kretschmann and Kröger [9].

In the following, we shall assume the presence of a very thin layer at the interface. The film is not necessarily homogeneous or isotropic, but its thickness d_f is such that $\eta = (\omega/c)d_f \ll 1$. The results obtained are first-order approximations, that is to say we neglect terms in η^2 and higher powers of this quantity.

The dispersion relation (2) is obtained by solving the equation $Z + Z_0 = 0$ with

$$Z = (\omega/c)\epsilon/\alpha \quad \text{and} \quad Z_0 = (\omega/c)\epsilon_0/\alpha_0 .$$

It can be shown [10] using the classical theory of thin films, that the presence of a very thin homogeneous film of dielectric constant $\epsilon_f = \epsilon_{f1} - i\epsilon_{f2}$ and thickness d_f leads to the following dispersion relation:

$$\frac{\partial(Z + Z_0)}{\partial x}\delta x = i\eta\left(\epsilon + \epsilon_0 - \frac{\epsilon\epsilon_0}{\epsilon_f} - \epsilon_f\right), \tag{10}$$

where x is the variable parameter (k or ω) and the value of the derivative is taken at the position of the resonance in the absence of the surface film, that is when $d_f = 0$. Here δx is the deviation of x from its value when $d_f = 0$. For an inhomogeneous film, for which ϵ_f is a function of z, we must replace $\epsilon_f d_f$ and d_f/ϵ_f by their average
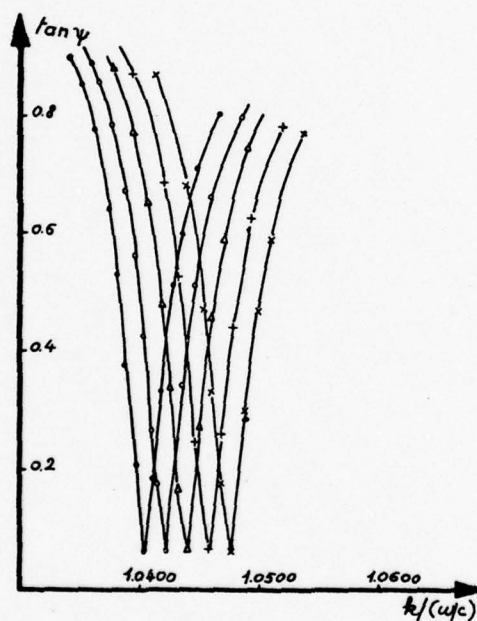

Fig. 4. Tan ψ versus $k/(\omega/c)$ at fixed frequency (λ = 5500 A) and variable incidence for the configuration of fig. 1b. The dielectric constants of the various media are $\epsilon_p = (1.464)^2$, $\epsilon = -13.46 - i\,0.6166$, $\epsilon_f = 4$ and $\epsilon_0 = 1$ and their thicknesses are d = 500 Å and d_f = 0, 5, 10, 15 and 20 A from left to right.

values

$$\int_0^{d_f} \epsilon_f(z)\,dz \quad \text{and} \quad \int_0^{d_f} dz/\epsilon_f(z)\,.$$

If the film is anisotropic uniaxial, with the optic axis in the z direction, its dielectric constants being ϵ_{fx} and ϵ_{fz}, we must substitute ϵ_{fz} in the $\epsilon_0\epsilon/\epsilon_f$ term and ϵ_{fx} in the ϵ_f term in eq. (10). We do not deal here with more complicated situations.

We discuss here mainly the situation where $x \equiv k$, i.e. a resonance at fixed frequency. Then $\delta x \equiv \delta k$ and we find, according to eq. (10) that

$$\frac{\delta k}{k_m} = \frac{\epsilon\epsilon_0}{(\epsilon_0 - \epsilon)(|\epsilon_0 + \epsilon|)^{3/2}}\left(\epsilon_0 + \epsilon - \frac{\epsilon_0\epsilon}{\epsilon_f} - \epsilon_s\right)\eta\,. \tag{11}$$

Here δk is the complex quantity introduced earlier [eq. (9)] to account for the modification of the ellipsometric response function due to a modification of the ϵ/ϵ_0 interface. In our approximation, δk is proportional to d. As we can write

$$\epsilon_0 + \epsilon - \epsilon_0\epsilon/\epsilon_f - \epsilon_f = (\epsilon_0 - \epsilon_f)(\epsilon_f - \epsilon)/\epsilon_f\,,$$
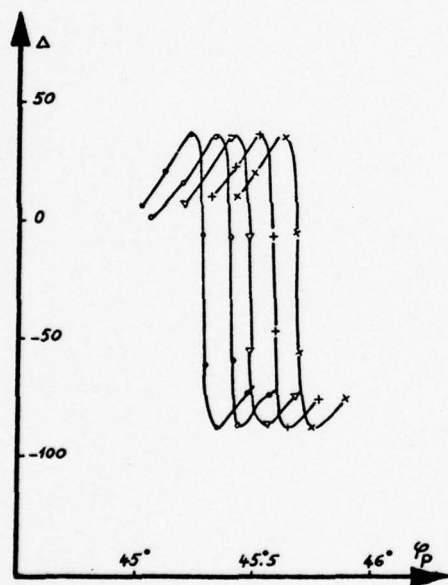

Fig. 5. Δ versus ϕ_p, the angle of incidence, for the same configuration and the same data as in fig. 4. Here k has been replaced by ϕ_p in order to show the experimentally encountered angular range corresponding to the SEW resonance.

it can be easily seen that, for $\epsilon_f < \epsilon$ and $0 < \epsilon_f < \epsilon_0$, δk is negative, the reverse being true for the other values of ϵ_f. These conclusions are drawn assuming that both ϵ and ϵ_f are essentially real ($\epsilon_{f2} \ll |\epsilon_{f1}|$). When ϵ_2 is very small and ϵ_f is real, $\delta k_2 \approx 0$ and $\delta k = \delta k_1$ is real. This means that the effect of the very thin film ϵ_f is a shift of the resonance from $k = k_{m1} + \Delta k_{m1}$ to $k = k_{m1} + \Delta k_{m1} + \delta k_1$ with practically no broadening at all. Figs. 4 and 5 give computed curves of tan ψ versus $k/(\omega/c)$ and Δ versus ϕ_0 for the Kretschmann configuration with $\epsilon_p = (1.464)^2$, $\epsilon = -13.46 - i\,0.6166$, $d = 500$ Å, $\epsilon_0 = 1$ and $\epsilon_f = 4$. The wavelength is kept fixed at $\lambda = 5500$ Å and the incidence is varied. The various curves from left to right correspond to $d_m = 0, 5, 10, 15$ and 20 Å. They show that δk is real for real ϵ_f and proportional to d_m. Indeed they are all identical and obtained from the curve corresponding to the bare interface ($d = 0$) by mere translations. Moreover, $\delta k = \delta k_1 > 0$, as expected from our considerations, because $\epsilon_f > \epsilon_0$. Another conclusion which can be drawn from these results is the impossibility of determining both ϵ_f and d_f from this type of experiments when the interfacial layer is very thin. On the other hand, the sensitivity of the method to the presence of such a layer is obviously much higher than when performing an ordinary ellipsometric measurement.

For the frequency ω_f for which $\epsilon_{f1} = 0$, $\epsilon(\omega_f) = -i\epsilon_{f2}$ and eq. (11) shows that

$$\frac{\delta k}{k} \simeq -i\,\frac{(\epsilon_0 \epsilon)^2}{(\epsilon_0 - \epsilon)(|\epsilon_0 + \epsilon|)^{3/2}}\,\frac{\eta}{\epsilon_2 f}. \tag{12}$$
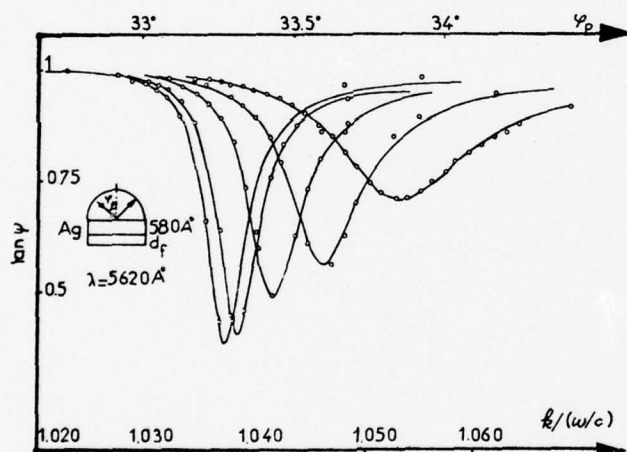

Fig. 6. Tan ψ versus $k/(\omega/c)$ for various stages of the tarnishing of a silver film ($d = 580$ A). Measurements performed at fixed frequency ($\lambda = 5620$ A) and variable incidence in the configuration of fig. 1b. Experimental points and full curves computed with the following data: $\epsilon_p = (1.89)^2$, $\epsilon = -14.36 - i\,0.6519$, $\epsilon_f = (2.9 - i\,0.4)^2$, $\epsilon_0 = 1$ and $d_f = 0, 2, 8, 16$ and 30 A from left to right (after ref. [7]).

Thus for $\omega = \omega_f$, δk is purely imaginary ($\delta k = -i\delta k_2$). The presence of a very thin film at the interface does not lead to a shift of the resonance, but only to a very strong damping. In fact, if ϵ_{2f} is very small ($\epsilon_{2f} \ll 1$), the damping can be so strong that the presence of the resonance can be hardly detected.

Figs. 6 and 7 show experimental results obtained during a SEW ellipsometric investigation of the tarnishing of a silver surface in the configuration of fig. 1b [7]. The SEW were excited by using a half-cylinder of dielectric constant $\epsilon_p = (1.89)^2$, the silver film was 580 Å thick and the experiments were performed at fixed frequency ($\lambda = 5620$ Å) and variable incidence, i.e. variable k. The tarnish layer had a dielectric constant $\epsilon_f = (2.9 - i\,0.4)^2$ and its thickness, corresponding to the various curves from left to right, were $d_f = 0, 2, 8, 16$ and 30 Å. The points are the experimental data and the full curves are the results of computation. Here $\epsilon_{fl} > \epsilon_0$ ($\epsilon_0 = 1$) and the shift of the resonance is towards larger k values ($\delta k_1 > 0$). The broadening of the resonance is apparent on the various curves. According to eq. (9), it is governed by the quantity $k_{m2} + \delta k_2 + \Delta k_{m2}$ and it increases with the thickness d_f of the tarnish film. From fig. 6, one notices that ψ_m increases with d_f. This is an immediate consequence of the relation

$$\tan \psi_m = \left| \frac{k_{m2} + \delta k_2 - \Delta k_{m2}}{k_{m2} + \delta k_2 + \Delta k_{m2}} \right|, \tag{13}$$

and of the fact that $d > d_m$ as can be seen from the presence of a maximum and a minimum in the Δ versus k curves (fig. 5).

This point is further emphasized in fig. 8, which reports experimental $\tan \psi$ and Δ versus $k/(\omega/c)$ for a gold film ($d = 408$ Å) in contact with a 1 N SO_4H_2 solution.
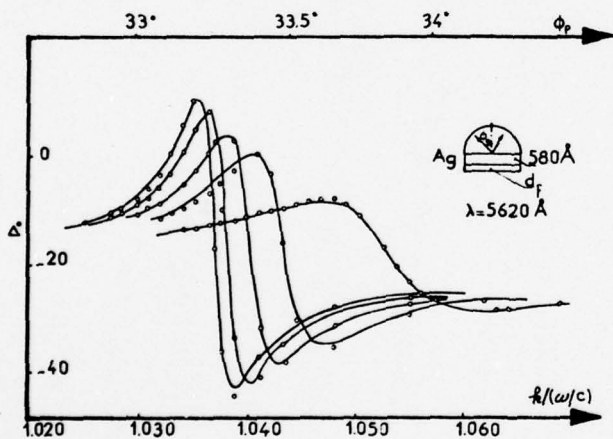

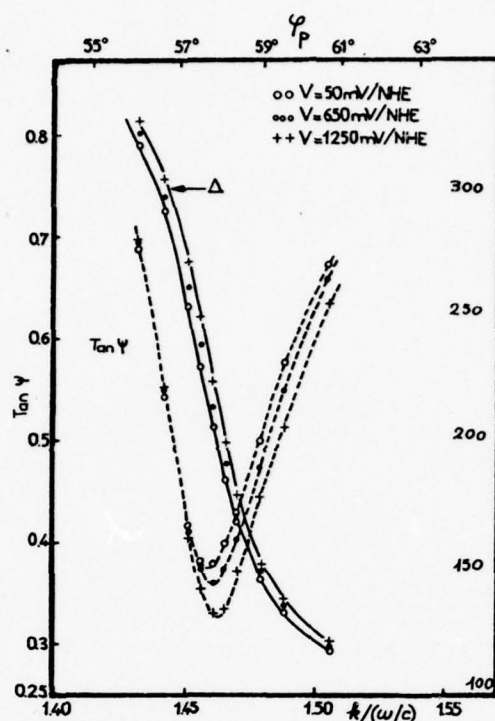Fig. 7. Δ versus $k/(\omega/c)$ for the same situations as in fig. 6.

Fig. 8. Tan ψ and Δ versus $k/(\omega/c)$ at fixed frequency (λ = 6093 A) and variable incidence in the Kretschmann configuration for an Au film (d = 408 A) in a 1 N H_2SO_4 solution for three different applied voltages.

The data were taken at λ = 6093 Å in the Kretschmann configuration for three different applied voltages: 0.05 V, 0.65 V and 1.25 V/NHE. The increasing modification of the interface is manifested through the shift and broadening of the resonance curves. The Δ curves show a monotonous variation (without maximum and minimum) indicating that $d < d_m$. Thus $k_{m2} < \Delta k_{m2}$ and ψ_m decreases now with increasing δk_2 according to eq. (13).

Let us now return to eq. (10) with $x \equiv \omega$, that is to say to experiments performed at fixed incidence and variable frequency. The shift $\delta\omega$ of the resonance is now given by

$$\delta\omega = \frac{2\epsilon^2[\epsilon_0 + \epsilon - (\epsilon\epsilon_0/\epsilon_f) - \epsilon_f]}{(\partial\epsilon/\partial\omega)(\epsilon_0 - \epsilon)(|\epsilon_0 + \epsilon|)^{1/2}} \eta . \tag{14}$$

The value of the derivative $\partial\epsilon/\partial\omega$ is taken at the frequency of the resonance in the absence of an interface film. The point to be noticed is the situation corresponding

to the case when $\epsilon_f = 0$ at the frequency ω_f of the resonance for the bare interface. Eq. (14) leads now to

$$(\delta\omega)^2 = \frac{-2\epsilon_0\epsilon^3}{(\epsilon_0 - \epsilon)(|\epsilon_0 + \epsilon|)^{1/2}(\partial\epsilon/\partial\omega)(\partial\epsilon_f/\partial\omega)}\,\eta\,. \tag{15}$$

This indicates a splitting of the dispersion curve. Instead of having a resonance at $\omega = \omega_f$, there are now two resonances at $\omega_f \pm \delta\omega$. The possibility of a splitting of the dispersion curve was first been pointed out by Agranovich and Malshukov [11]. Usually $\delta\omega = \delta\omega_1 + i\delta\omega_2$ is a complex quantity. For $\omega = \omega_f$, $\delta\omega$ is practically a purely imaginary quantity, indicating a strong damping of the resonance, which disappears and is replaced by the two dips in the $\tan\psi$ versus ω curve at $\omega = \omega_f \pm \delta\omega$.

Let us now return briefly to the case of a very thin inhomogeneous layer. A situation which corresponds to the occurrence of two superimposed very thin layers is found in the investigation of the metal–electrolyte interface. Abelès et al. [12] have studied the $Au-H_2SO_4$ and $Au-HClO_4$ interfaces by optically exciting SEW and using ellipsometric detection. The results obtained at fixed frequency ($h\omega = 2.034$ eV) for different values of the potential of the Au electrode (film) were interpreted by using a model in which both the electrolyte and the metal electrode are altered by the applied voltage. According to eq. (11), if δk_a and δk_b correspond to the modifications occurring in the metal and in the electrolyte respectively, then $\delta k = \delta k_a + \delta k_b$. If we assume that the modified very thin region at the surface of the electrolyte is non absorbing, which is a reasonable standard assumption, then $\delta k_2 = \delta k_{a2}$ because $\delta k_{b2} \approx 0$. Thus δk_2 provides information on the altering of the surface region in the metal. From this, one can compute δk_{a1} and deduce $\delta k_{b1} = \delta k - \delta k_{a1}$, i.e. the modification of the electrolyte. This is probably the first detailed investigation of an inhomogeneous very thin layer and it shows how SEW enabled to distinguish the effects of the applied field in the electrolyte and in the metal.

6. Concluding remarks

The aim of this presentation was: (a) to introduce the reader to SEW, (b) to indicate how they can be generated and ellipsometrically detected, (c) to stress their usefulness for the investigation of surfaces and interfaces. The examples chosen correspond to the situation where the surface active medium is a quasi-free electron plasma. The theoretical results can be used to interpret measurements on surface polaritons in the infrared too. The only problem is purely technical, because infrared ellipsometry is still in its infancy.

The given examples are all obtained in the Kretschmann configuration (fig. 1b), but, as already stated above, those corresponding to the configuration of fig. 1a would be absolutely similar. The choice was governed by the fact that the author has used the former only.

We did not show any dispersion curve (ω versus k). This is due to the fact that ellipsometric measurements yield $k = k_{m1}(\omega) + \Delta k_{m1}(\omega)$, whereas the dispersion relation reads $k = k_{m1}(\omega)$. A direct determination of the dispersion curve is very difficult, because we ought to have $\Delta k_{m1}(\omega) = 0$, i.e. to suppress any coupling between the prism and the surface propagating SEW, which means that the contrast (or intensity) of the resonance would be exceedingly small. This can be also seen from eqs. (7) and (8), where $\Delta k_{m2}(\omega) = 0$ due to the fact that d is very large. An indirect determination of the dispersion curve can be achieved by first measuring ϵ and ϵ_0 and then using eq. (2). If ϵ_0 is assumed frequency independent and well known, the only remaining problem is the determination of $\epsilon(\omega)$. This can be achieved, for instance, from measurements of ψ and Δ at fixed frequency and variable incidence. Roughly speaking, the position, the intensity and the width of the resonance provide the necessary information for the determination of $\epsilon = \epsilon_1 - i\epsilon_2$ and d. Results obtained using measurements of p-polarized light reflectivity have been given by Kretschmann [6] and Otto and Sohler [13].

The discussion of the influence of a very thin layer on SEW given in section 5 shows that the observed resonance can be quite different when working at fixed frequency or at fixed angle of incidence. In the first instance, one observes a modification of the resonance (shift, broadening, drop of intensity), whereas when working at fixed incidence, a splitting of the resonance can occur. Differences in the observed effects for the two types of scanning have also been observed in the region of rather large absorption in the surface active material [14,15].

References

[1] J. Zenneck, Ann. Physik (Leipzig) 23 (1907) 846.

[2] A. Sommerfeld, Ann. Physik (Leipzig) 28 (1909) 665.

[3] E. Burstein, W.P. Chen, Y.J. Chen and A. Hartstein. J. Vacuum Sci. Technol. 11 (1974) 1004.

[4] E.N. Economou and K.L. Ngai, in: Advances in Chemical Physics, Vol. 27, Eds. I. Prigogine and S.A. Rice (Wiley, New York, 1974) p. 265.

[5] A. Otto, Z. Physik 216 (1968) 398.

[6] E. Kretschmann, Z. Physik 241 (1971) 313.

[7] F. Abelès and T. Lopez-Rios, in: Polaritons, Proc. the 1st Taormina Research Conf. on the Structure of Matter, Eds. E. Burstein and F. de Martini (Pergamon, New York, 1974) p. 241.

[8] A.J. Braundmeier and E.T. Arakawa, J. Phys. Chem. Solids 35 (1974) 517.

[9] E. Kretschmann and E. Kröger, J. Opt. Soc. Am. 64 (1975) 150.

[10] F. Abelès, Thin Solid Films, to be published.

[11] V.M. Agranovich and A.G. Malshukov, Opt. Commun. 11 (1974) 169.

[12] F. Abelès, T. Lopez-Rios and A. Tadjeddine, Solid State Commun. 16 (1975) 843.

[13] A. Otto and W. Sohler, Solid State Commun. 16 (1975) 1319.

[14] E.T. Arakawa, M.W. Williams, R.N. Hamm and R.H. Ritchie, Phys. Rev. Letters 31 (1973) 1127.

[15] R.W. Alexander, G.S. Kovener and R.J. Bell, Phys. Rev. Letters 32 (1974) 154.

Critique

F. Meyer: I wonder can you talk about a plasma frequency for a very dilute monolayer?

F. Abelès: If these waves are very sensitive to the surface they should also be sensitive to the roughness of the surface. In all we done we have an ideally smooth surface. The important thing is that by exciting surface electromagnetic waves you can have scattered light in the medium of total reflection where otherwise there is nothing. Concerning the plasma frequency, you are obtaining a kind of a zero of the dielectric constant of the material you have on top of the surface. In fact the only assumption is that the dielectric constant becomes zero.

D.E. Aspnes: Could you amplify slightly on your earlier statement concerning the wavelength range in which this technique is applicable? I believe you said it could be used whenever the dielectric function is essentially negative. Can you make that, for example, everywhere negative?

F. Abelès: You can use it at frequencies where the real part of the dielectric constant is negative and in absolute value larger than the dielectric constant of the other epsilon b material.

J. Kruger: This would seem to be a good technique for trying to learn something about the double layer. Are you planning such an experiment? I think it would be very worthwhile.

F. Abelès: Yes, in fact we are starting some experiments on that and we hope to be able to continue. We found it very sensitive and at the same time non-destructive. The measuring beam comes from outside, from one region, you can see what happens in the cell on the other side. We studied anodic oxidation of gold, at potentials high enough for oxidation. We also measured the dielectric constant of gold hydroxide on the surface.

N.M. Bashara: Could you amplify a little more on the very thin layer of silver experiment?

F. Abelès: This was a computed case. We didn't do the experiment. When you have the zero of the dielectric constant of a very thin film on silver corresponding to the position of the resonance on the free silver surface, you have a striking effect. This has been very recently measured by Russian workers using reflectance measurements in the infrared. I have seen a preprint but the results are not yet published.

APPENDIX II

Spectroscopy of Very Thin Metal Layers on Metallic Surfaces Using Optical Excitation of Surface Plasmons (*).

T. LOPEZ-RIOS and G. VUYE

Laboratoire d'Optique des Solides (**), *Université Paris VI*
4 Place Jussieu - 75230 Paris Cedex 05, France

Summary. — We show how the optical constants of very thin layers deposited on metallic surfaces can be deduced from the modifications of the R_p resonances due to excitation of surface plasma waves by the ATR method. The optical constants of discontinuous Au thin layers (thickness < 20 Å) on Ag surfaces, prepared and studied under ultra-high vacuum, are determined over the $(4000 \div 6000)$ Å spectral range.

Optical spectroscopy (reflection and transmission measurements), which is widely used for studying the optical properties of solids, is not as powerful when applied to surface investigations, because of its lack of sensitivity to surface phenomena. It was shown that surface plasma waves (SPW) are very sensitive to surface phenomena and can be employed as a tool to study surfaces [1,2] and interfaces [3]. Till now, most of the work was done for few frequencies only. We present here, as an example, results of optical spectroscopy using SPW of very thin deposits of gold (~ 10 Å) on silver surfaces. It must be underlined that the determination of the optical constants of very

---

(*) Paper presented at the «Taormina Research Conference on Recent Developments in Optical Spectroscopy of Solids», held in Taormina, September 1976.
(**) Equipe de Recherche Associée au C.N.R.S.
(¹) K. HOLST and H. RAETHER: *Opt. Comm.*, **2**, 312 (1970).
(²) F. ABELÈS and T. LOPEZ-RIOS: *Proceedings of the Taormina Conference on Structure of Matter «Polaritons»*, edited by E. BURSTEIN and F. DE MARTINI (New York, N.Y., 1974), p. 241.
(³) F. ABELÈS, T. LOPEZ-RIOS and A. TADJEDDINE: *Sol. State Comm.*, **16**, 843 (1975).

823

thin films on highly reflecting substrates (like silver in the visible region) is
particularly difficult by other methods.

SPW are excited by the classical ATR method in the Kretschmann config-
uration (prism-metallic film (typically 500 Å thick)-vacuum). In our experi-
ments, the silver films as well as the gold surface layers are deposited under
ultra-high vacuum, and the optical measurements performed *in situ* under
the same vacuum with the help of an especially built double-beam spectro-
photometer. We measure the square of the reflection coefficient for p-polarized
light as a function of wave-length for different angles of incidence at room
temperature. The mass thickness of the films is determined with a Sloan
oscillating quartz. The 500 Å silver films are made of regular crystallites with
lateral dimensions of a few 1000 Å and present a fiber structure with the (1, 1, 1)
planes parallel to the substrate. The free surface is close to an assembly of
(1, 1, 1) terraces [4].

In the present experiments, we fix the angle of incidence φ and we record
R_p^2 *vs.* the wave-length λ. Figure 1 shows a recording of $R_p^2(\lambda)$ around the
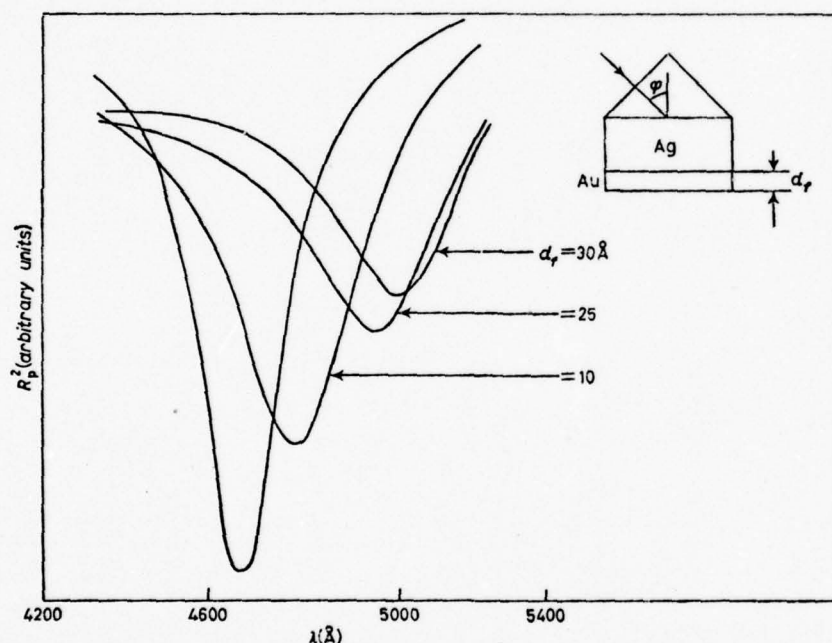SPW resonance for $\varphi = 46.5°$, for a silver thin film (658 Å thick), and the

Fig. 1. – R_p^2 *vs.* λ (arbitrary units) for a silver film (658 Å thick) and for thin gold
layers of mass thickness 10, 25 and 30 Å deposited on the free silver surface. The
internal angle of incidence was $\varphi = 46.5°$.

[4] M. GANDAIS, V. NGUYEN VAN and S. FISSON: *Thin Solid Films*, **15**, 843 (1973).

progressive modification of this curve produced by gold deposits of increasing
mass thickness condensed on the free silver surface. One can observe a shift
and a broadening of the resonance. We have repeated such recording for several
angles of incidence in order to obtain the resonances in R_p as a function of the
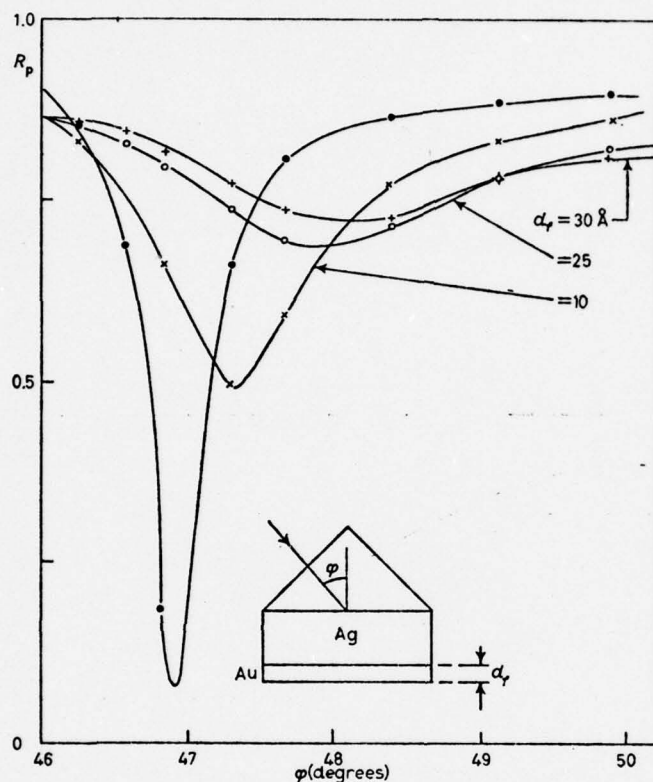angle of incidence. Figure 2 shows $R_p(\varphi)$ for $\lambda = 4563$ Å for the same experi-

Fig. 2. – R_p *vs.* φ for the same experimental situation as in fig. 1. $\lambda = 4563$ Å.

mental situation as in fig. 1. Here again the gold surface layer gives rise to
an angular shift and a broadening of the resonance, the latter being related
to the absorption in the layer. From the shift of the resonance, we can obtain
the real part of the modification of the surface plasmon wave vector ΔK_1 and,
from the broadening, its imaginary part ΔK_2. From the λ values corresponding
to the minimum of R_p for each angle of incidence, we deduce the surface plasmon
dispersion relations for the free silver surface and for silver covered by thin
gold layers.

All physical information about the surface layer comes from ΔK_1 and ΔK_2
and, if we know the thickness d_f of the surface layer, we can compute its optical

constants $\varepsilon_f = \varepsilon_{f1} + i\varepsilon_{f2}$ from the modification of the resonance in $R_p(\varphi)$. In fact, there are always two solutions, but only one of them has a physical meaning; the accuracy in this determination is quite good.

Using the exact electromagnetic formula for multilayer systems ([5]), we have computed the optical constants for the gold surface layers on silver by a least-square fitting of the $R_p(\varphi)$ curves for each wave-length, the thickness of d_f being taken equal to the value given by the oscillating quartz.

Figure 3 shows the values of ε_{f1} and ε_{f2} between 4000 and 6000 Å for thin layers of Au on Ag with $d_f = 13$ and 27 Å. It is found that the values of ε_{f1} over the whole spectral range are independent of d_f, are negative and are very close to the optical constants determined by accurate measurements on well-crystallized thicker Au films ([6]). We have an analogous situation for ε_{f2}; nevertheless, the errors are more important (they are essentially related to errors on ΔK_2). It must be emphasized that the absolute values of ε_f may depend appreciably on the values chosen for d_f, but the general shape of the curves remains the same. In any case, we find ε_f values close to the bulk values within our experimental uncertainties for layer thicknesses from 10 to 40 Å.
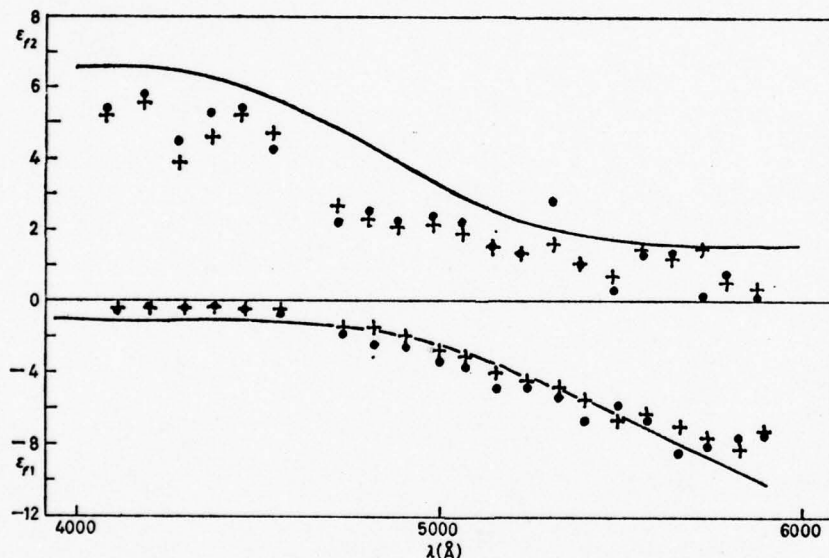

Fig. 3. – Values of ε_{f1} and ε_{f2} for gold surface layers (13 (•) and 27 (+) Å thick) deposited on free silver surface. The continuous line corresponds to the bulk values for Au taken from ref. ([6]).

([5]) F. ABELÈS: in *Advanced Optical Techniques*, edited by A. C. S. VAN HEEL (Amsterdam, 1967), p. 144.
([6]) M. L. THEYE: *Phys. Rev. B*, **2**, 3060 (1970).

It is known ([7]) that the growth of gold deposits on (1, 1, 1) silver surfaces at room temperature is very discontinuous. Electron-microscope investigations have shown that our deposits are formed by islands, the thickness of which is of the order of their lateral dimensions. For a deposit corresponding to $d_f = 13$ Å, it was found that the island diameter is about 60 Å with a density of about $4 \cdot 10^{11}/\text{cm}^2$. The island dimensions increase with the thickness d_f, reaching 100 to 200 Å for d_f of the order of 40 Å.

The observation that ε_f equals the bulk values for very discontinuous layers with island dimensions from 200 to 60 Å suggests that the model of a continuous layer is valid in all cases and that roughness effects are not very important.

In conclusion, this new method should be very useful to study various surface phenomena like chemisorption or oxidation on metals as well as, with a minor modification, diffusion of atoms or molecules through metallic films ([8]).

* * *

([7]) J. G. ALLPRESS and J. V. SANDERS: *Phil. Mag.*, **9**, 645 (1964).
([8]) F. ABELÈS and T. LOPEZ-RIOS: *Opt. Comm.*, **11**, 89 (1974).

● RIASSUNTO (*)

Si mostra come le costanti ottiche di strati molto sottili depositati su superfici metalliche possano essere dedotti dalle modificazioni delle risonanze R_p dovute all'eccitazione di onde del plasma di superficie per mezzo del metodo ATR. Si determinano le costanti ottiche di strati sottili discontinui di Au (spessore < 20 Å) su superfici di argento, preparate e studiate nell'ultravuoto, nell'intervallo spettrale tra 4000 e 6000 Å.

(*) *Traduzione a cura della Redazione.*

Спектроскопия очень тонких металлических слоев на металлических поверхностях, используя оптическое возбуждение поверхностных плазмонов.

Резюме (*). — Мы показываем, как оптические постоянные очень тонких слоев, нанесенных на металлические поверхности, могут быть получены из преобразований R_p резонансов, благодаря возбуждению поверхностных плазменных волн с помощью ATR метода. В спектральной области (4000÷6000) Å определяются оптические постоянные дискретных золотых тонких слоев (толщина < 20 Å) на серебряных поверхностях, приготовленных и исследованных при ультравысоком вакууме.

(*) *Переведено редакцией.*

APPENDIX III

_____

Appendix III which DDC cannot furnish be-
cause of illegibility can be secured on the
open market per A. Putman, USAR&SG (Europe)

APPENDIX IV

MODIFICATION OF THE DISPERSION RELATIONS FOR SURFACE PLASMONS
BY VERY THIN SURFACE FILMS IN THE VICINITY OF THEIR PLASMA FREQUENCY

T. LOPEZ-RIOS

Laboratoire d'Optique des Solides[*], *Université Paris VI,*
4 Place Jussieu, 75230 Paris Cedex 05, France

Received 1 February 1976

Dispersion curves are calculated for a situation corresponding to a very thin K film on Al. The vicinity of the plasma frequency of the film is thoroughly investigated and the influence of absorption in the film is stressed. The gap in the dispersion curve computed at constant frequency disappears with increasing absorption in the film. Experimental possibilities for investigating very thin films by ATR are discussed and an approximate expression for the predicted splitting of the minimum of the reflectance for p-polarized light is given. The splitting is shown to be independent of the absorption in the film.

1. Introduction

The dispersion relations for surface polaritons [1, 2] and surface plasmons (SP) [3] have already been discussed by several authors, even for multilayer systems. We shall discuss here the situation where a very thin metal film is supported by a metallic substrate propagating surface waves at its interface with vacuum or a dielectric. The modification of the surface waves due to the alteration of the metal surface can provide information about surface phenomena like chemisorption, metallic adsorption or oxidation.

In the general case, the presence of a very thin film (thickness $d_f \ll$ wavelength λ) at the metal–dielectric interface leads to a shift of the dispersion curve (frequency ω versus k, the projection of the wavevector along the interface) and a broadening related to the absorption of the film. The analysis of the influence of the film can be performed by using a first order approximation (linear in $k_0 d_f$, with $k_0 = \omega/c$), therefore the modifications of k are proportional to the film thickness. This approximation breaks down when $k/k_0 \gg 1$ and $(k/k_0)k_0 d_f$ is no more a small quantity. Such a situation is not encountered in optical experiments using the SP excitation by attenuated to-

[*] Equipe de Recherche Associée au C.N.R.S.

tal reflection (ATR) [4,5]. The linear approximation has already been used for the investigation of surface [6] and interface [7] modifications.

Another case where the first-order approximation may be questioned, corresponds to the frequencies for which the dielectric function of the film (ϵ_f) goes to zero or to infinity. For ionic crystals, this occurs at ω_{LO} and ω_{TO} (longitudinal and transverse optical phonon frequencies) respectively. This situation has been discussed by Agranovich et al. [8] and it leads to a splitting of the surface polaritons. Experimental evidence for this has been provided by Yakovlev et al. [9] who have investigated LiF films on sapphire (Al_2O_3) and rutile (TiO_2). For metals, this occurs at the plasma frequency ω_p. Economou et al. [3] have discussed the dispersion curve corresponding to a metal film on a metal substrate, but only for the case corresponding to real values of k.

We present here an analysis for the same situation (metal film on metal substrate), but we discuss important effects due to the damping (absorption) in the film. In addition, we investigate both real and complex values of k, pointing out the differences observed in experiments conducted either at fixed k/k_0 and variable ω or at fixed ω and variable k/k_0, and we present curves showing the expected behavior of the reflectance for p-polarized light (R_p) measured at

fixed incidence and variable ω in an ATR configuration. The computations were performed in the case of a K film on Al. They do not take into account possible (and probable) spatial dispersion effects.

2. Dispersion relations

Let $\epsilon = \epsilon_1 - i\epsilon_2$ and ϵ_0 be the dielectric functions of a metallic plasma and of a dielectric, which are in contact. The condition for occurrence and propagation of an SP at the ϵ/ϵ_0 interface is given by $Z + Z_0 = 0$, where Z and Z_0 are the optical admittances of a p-polarized wave in both media, with $Z = \epsilon \times (\epsilon - S^2)^{-1/2}$ and $Z_0 = \epsilon_0(\epsilon_0 - S^2)^{-1/2}$ and $S = k/k_0$. It is well known [1] that this condition leads to the dispersion relation

$$S^2 = (k/k_0)^2 = \epsilon\epsilon_0/(\epsilon + \epsilon_0) \tag{1}$$

where ϵ is a function of ω and ϵ_0 is assumed to be frequency independent.

The presence of a thin film at the ϵ/ϵ_0 interface leads to a modified condition for the occurrence and propagation of SP, namely [10,11]

$$Z + Z_0 + (ZZ_0/Z_f + Z_f) \tanh \varphi = 0, \tag{2}$$

with $Z_f = \epsilon_f(\epsilon_f - S^2)^{-1/2}$ and $\phi = k_0 d_f(S^2 - \epsilon_f)^{1/2}$. SP can be excited by working either at fixed frequency and variable S or at fixed S and variable frequency. It has been shown by Alexander et al. [12] that the dispersion curves obtained at the ϵ/ϵ_0 interface in these two cases coincide only when $\epsilon_2 = 0$. In order to show the effect of a very thin layer on SP in the vicinity of its plasma frequency $\omega_{pf} = 2\pi c/\lambda_{pf}$, we have chosen an example corresponding to a K film ($d_f = 20$ Å) on Al. The dielectric constants of the two metals are given by the Drude expressions:

$$\epsilon = 1 - \omega_p^2/\omega^2(1 - i/\omega\tau),$$

$$\epsilon_f = 1 - \omega_{pf}^2/\omega^2(1 - i/\omega\tau_f),$$

with $\lambda_p = 2\pi c/\omega_p = 837$ Å, $h\omega_p = 14.88$ eV, $\omega_p\tau = 24.85$ for Al [13], $\lambda_{pf} = 3260$ Å, $h\omega_{pf} = 3.80$ eV, for K [14] and different values of the relaxation time for the conduction electrons in the film: $\omega_{pf}\tau_f = 10$ and 50, τ_f being strongly dependent on the crystalline structure of the film. We explore the region of frequencies comprized between $0.8\omega_{pf}$ and $1.2\omega_{pf}$,
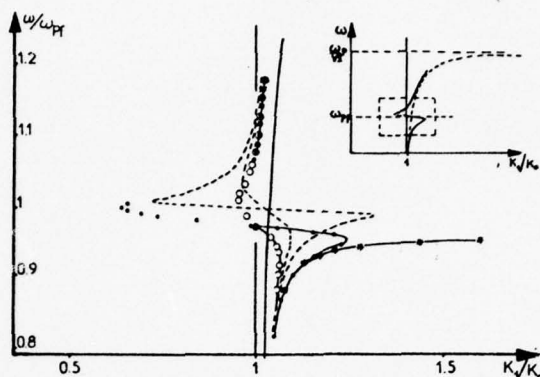

Fig. 1. ω/ω_{pf} versus k_1/k_0 obtained from eq. (2) (for ω real and k complex) for a K film ($d_f = 20$ A, $h\omega_{pf} = 3.80$ eV [14]) on Al ($h\omega_p = 14.88$ eV, $\omega_p\tau = 24.85$ [13]). The open circles, the full circles and the stars correspond to $\omega_{pf}\tau_f = 10, 50$ and infinity, respectively. The dashed lines are computed in the linear approximation according to eq. (3). The full continuous line corresponds to a bare Al surface. The insert contains a schematic dispersion curve for frequencies up to $\omega_p/2^{1/2}$.

in which the influence of the surface layer ϵ_f is the most important.

Figs. 1 and 2 show the solution of eq. (2) for real values of ω and complex values of $S = k/k_0 = S_1 - iS_2 = (k_1 - ik_2)/k_0$. Fig. 1 displays the relation between ω and the real part of k/k_0, i.e. S_1. In our notation, the light line corresponds to $S_1 = 1$ and it is represented by a vertical straight line. The dispersion relation corresponding to bare Al in contact with vacuum (ϵ/ϵ_0 interface) is represented by a continuous line.
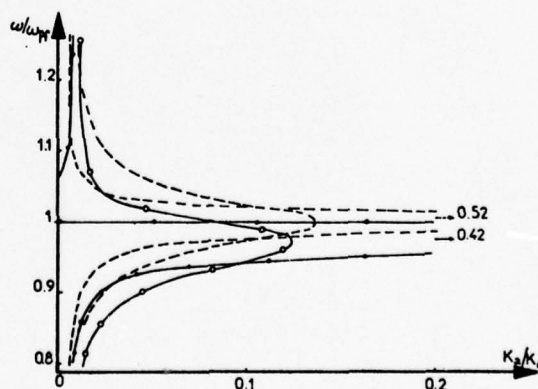

Fig. 2. ω/ω_{pf} versus k_2/k_0 for the same situations and with the same notations as in fig. 1.

343

It is a smooth curve close to the light line over the frequency range of interest: $0.8\omega_{pf}$ to $1.2\omega_{pf}$. The curves corresponding to the presence of a very thin K film are characterized by an important backbending which is strongly dependent on the absorption in the film (i.e. on the value of τ_f).

When $\epsilon_{f2} = 0$, there are two distinct branches going to the limit values $\omega = \omega_{pf}/2^{1/2}$ and $\omega = \{(\omega_p^2 + \omega_{pf}^2)/2\}^{1/2}$ corresponding to SP at the K–vacuum interface and at the Al–K interface respectively. When $\epsilon_{f2} \neq 0$, the dispersion curves show backbending. For large absorption, the two distinct branches are no longer observed and the curves are continuous. The dispersion curves have been drawn on both sides of the light-line $S_1 = 1$. For $S_1 > 1$ we have true SP, whereas for $S_1 < 1$ we do not have evanescent waves in the vacuum. This case is referred to in the literature [15] as leading to leaky Fano modes at the surface. For large damping in the surface layer (τ_f small), the whole dispersion curve is situated to the right of the light-line, that is $S_1 > 1$.

Fig. 2 displays the relation between ω and the imaginary part of k/k_0, i.e. S_2. Both curves corresponding to $\omega_{pf}\tau_f = 10$ and 50 show a maximum for $\omega \simeq \omega_{pf}$, the intensity of which decreases with increasing damping. As the propagation length of an SP along the surface, L, is related to S_2 through $L = \lambda/2\pi S_2$, it is clear that L reaches a minimum at $\omega \simeq \omega_{pf}$. It should be noticed that the curve with stars in fig. 1 also corresponds to the solutions of eq. (2) with real S and complex $\omega = \omega_1 + i\omega_2$, even when $\epsilon_{f2} \neq 0$ because these solutions are almost insensitive to absorption.

Another important point to be made is that for large values of τ_f (small absorption in the surface layer), there is a gap in the dispersion curve. In our case, this can be seen on the curves giving ω versus S_1 and ω versus S_2 (figs. 1 and 2) for $\omega_{pf}\tau_f = 50$. There is no gap for $\omega_{pf}\tau_f = 10$. There is nothing equivalent when solving eq. (2) for real S and complex ω.

These results can be understood, at least qualitatively, by looking for an approximate solution of eq. (2), corresponding to the approximation $\tanh \phi \approx \phi$. In this linear approximation one finds that, if k is given by eq. (1), then the solution of eq. (2) is given by $k + \delta k$ with [6,11]

$$\delta k = k^2 \frac{(-\epsilon_0\epsilon)^{1/2}}{\epsilon_0 - \epsilon} \left[1 - \left(\frac{k}{k_0}\right)^2 \left(\frac{1}{\epsilon_f} + \frac{\epsilon_f}{\epsilon\epsilon_0}\right) \right] d_f. \qquad (3)$$

344

The dispersion curves computed according to eq. (3) are represented by dashed lines in figs. 1 and 2. They are similar to the curves computed exactly from eq. (2) and discussed above, the slight shift of their inflexion point (in fig. 1), or peak (in fig. 2) being due to a breakdown of the linear approximation in the immediate vicinity of ω_{pf}.

The optical excitation and detection of SP is usually performed using an ATR configuration. As stressed before, the experiments can be conducted either at fixed frequency and variable incidence or at fixed incidence and variable frequency. In the former case, it appears from fig. 1 that there is one and only one point on the dispersion curve which is reached for each frequency. When working at fixed incidence, that is to say at constant k/k_0, there are always two points on the dispersion curve which are reached for two different frequencies: the intersection of the line $k/k_0 =$ const. with the dispersion curve in a ω_1 versus k/k_0 representation (this curve is identical to the curve with stars in fig. 1). In a first-order approximation, the distance between them has been given by Abelès [11]. In our case, with $\omega_p \gg \omega_{pf}$, its approximate expression is

$$\delta\lambda/\lambda_{pf} = \pm (\pi d_f/\lambda_p)^{1/2} \qquad (4)$$

which shows that even for very small thicknesses of the surface film, $\delta\lambda$ can be easily measured. Fig. 3 shows the computed curves for R_p versus λ in an ATR experiment at fixed incidence using the indicated con-
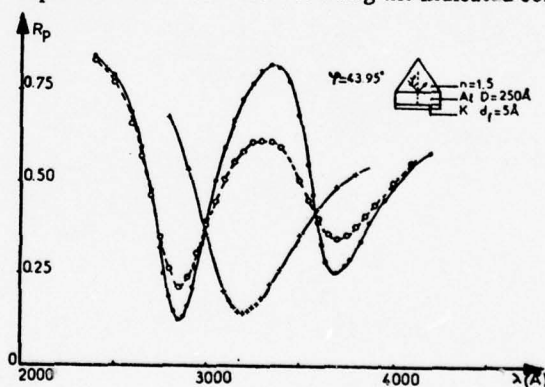

Fig. 3. Computed values of the reflectance for p-polarized light, R_p, in an ATR configuration schematically shown in the insert for an Al surface covered with a very thin K film ($d_f = 5$ A) and for different values of the absorption in the film (open circles: $\omega_{pf}\tau_f = 10$, full circles: $\omega_{pf}\tau_f = 50$). The crosses give the values of R_p for a bare Al surface.

figuration. The values of λ corresponding to the minima of R_p give the positions of the points on the dispersion curve corresponding to the given incidence $\phi = 43°95$. The curve joining the crosses is for an Al—vacuum interface, the two other curves representing the effect of a very thin K film ($d_f = 5$ Å) on Al. The curves with full and open circles correspond to $\omega_{pf}\tau_f$ = 50 and 10 respectively. It is apparent that the positions of the minima are not dependent on the absorption in the K film, which only causes a broadening of the resonance.

3. Conclusion

For a thin metal film on a metal substrate, we have discussed the influence of the absorption in the film on the SP dispersion curves. The presence of a gap in the curve computed for real ω and complex k is strongly dependent on the absorption in the film, the gap vanishing for strong absorption. It has been shown that for a very thin film of K on Al ($d_f = 5$ Å), a rather large (800 Å) splitting of the SP resonance in an ATR experiment conducted at fixed incidence takes place in the vicinity of the plasma frequency of the film, the resonance frequency being independent of the absorption (τ_f) in the film. An approximate expression allowing a rapid estimate of the splitting has been given. It is clear that films as thin as 1 Å ought to be easily detected by this method.

Acknowledgement

References

[1] E. Burstein, W.P. Chen, Y.J. Chen and A. Hartstein, J. Vac. Sci. Technol. 11 (1974) 1004.
[2] C.A. Ward, R.W. Alexander and R.J. Bell, Phys. Rev. B 12 (1975) 3293.
[3] E.N. Economou, Phys. Rev. 182 (1969) 539;
    K.L. Ngai and E.N. Economou, Phys. Rev. B 4 (1971) 3132.
[4] A. Otto, Z. Physik 216 (1968) 398.
[5] E. Kretschmann, Z. Physik 241 (1971) 313.
[6] F. Abelès and T. Lopez-Rios, in: Polaritons, Proc. 1st Taormina Res. Conf. Structure of Matter, ed. by E. Burstein and F. de Martini (Pergamon, New York, 1974) p. 241.
[7] F. Abelès, T. Lopez-Rios and A. Tadjeddine, Solid State Commun. 16 (1975) 843.
[8] V.M. Agranovich and A.G. Malshukov, Opt. Commun. 11 (1974) 169.
[9] V.A. Yakovlev, V.G. Nazin and G.N. Zhizhin, Opt. Commun. 15 (1975) 293.
[10] E.N. Economou and K.L. Ngai, in: Advances in Chemical Physics, ed. by I. Prigogine and Stuart A. Rice, p. 298.
[11] F. Abelès, Thin Solid Films, to be published.
[12] R.W. Alexander, G.S. Kovener and R.J. Bell, Phys. Rev. Lett. 32 (1974) 154.
[13] W.R. Hunter, J. Physique 25 (1964) 154.
[14] N.V. Smith, Phys. Rev. B 138 (1969) 634;
    J. Monin and G.A. Boutry, Phys. Rev. B 9 (1974) 1309.
[15] E. Burstein, A. Hartstein, J. Schoenwald, A.A. Maradudin, D.L. Mills and R.F. Wallis, in: Polaritons, Proc. 1st Taormina Res. Conf. Structure of Matter, ed. by E. Burstein and F. de Martini (Pergamon, New York, 1974) p. 241.

APPENDIX V

_____

1

SPLITTING OF THE Al SURFACE PLASMONS DISPERSION CURVES BY
Ag SURFACE LAYERS

DEDOUBLEMENT DES COURBES DE DISPERSION DES PLASMONS DE SURFACE
DE L'Al PRODUIT PAR DES COUCHES SUPERFICIELLES D'Ag

T. LOPEZ-RIOS, F. ABELES and G. VUYE
Laboratoire d'Optique des Solides
Equipe de Recherche Associée au CNRS n° 462
Université Pierre et Marie Curie
4, place Jussieu
75230 Paris Cedex 05
France

Abstract

The effects of very thin Ag surface layers on the propagation
of surface plasma waves (S.P.W.) excited by ATR at an Al surface
are investigated in the vicinity of the Ag plasma frequency and
the S.P.W. dispersion relations are obtained. A splitting of
the dispersion curves is found for Ag layers 26, 39 and 58 Å
thick, but does not appear for thinner layers. Experimental
and computed dispersion curves are compared.

Résumé

On étudie les effets de films très minces d'argent sur la
propagation d'ondes de plasma de surface excitées par réflexion
totale atténuée à la surface de l'aluminium. On examine surtout
le domaine spectral voisin de la fréquence de plasma correspon-
dant à l'argent et l'on en déduit les relations de dispersion
pour les ondes de plasma de surface. On trouve un dédoublement
des courbes de dispersion pour des films d'argent d'épaisseurs
26, 39 et 58 Å, mais ce dédoublement n'existe pas pour les films
plus minces. On compare les courbes de dispersion calculées à

1.   Introduction

Since the pioneering work of Ritchie (1) and Ferrell (2),
the existence of coupled surface plasmon modes in metallic slabs
is well established. Such coupled modes have recently been
observed by low-energy electron energy loss spectroscopy for
an Al film of atomic dimension on CdSe and CdS (3). When the
two surrounding media are of different nature and when the
thickness of the metallic film is large enough, the modes are
nearly decoupled and tend towards the two surface plasmon modes
corresponding to the two interfaces (4, 5). For metallic films
on metal surfaces, one mode is related to the surface plasmon
at the metal/metal interface. The existence of such interface
plasmon modes was first suggested by Stern and Ferrell (6) but
up to now, to our knowledge, there is no evidence for them from
optical experiments. Surface plasma waves (SPW) should indeed
exist at the metal/metal interface for free electron metals in
a spectral range corresponding to the reflecting region for one
metal, and to the region with positive dielectric constant for
the other one.

An interesting situation occurs when the thickness d_f of
the metallic film deposited on a metal substrate becomes very
small, i.e. much smaller than the wavelength of excitation.
In the small wave-vector range, the two modes are strongly
coupled and the effect of a surface metallic layer, having a
well-defined plasma frequency in the spectral region where
the substrate can propagate SPW, is a splitting in the surface
plasmon dispersion relation. The two branches of the mixed
modes should be detected in an ATR experiment (7).

Very recently, mention was made of a new branch in the
surface plasmon dispersion curve induced by an inhomogeneous
charge distribution at a metallic surface (8, 9). This upper
branch, related to surface inhomogeneity, should exist for an
accumulation charge layer as well as for a depletion layer (10).

Guidotti and Rice (11) claim to have found this new branch in
the case of Hg-Cd alloys; this is, up to now, the only experi-
mental evidence for it. Here, we report on ATR experiments
performed on very thin Ag films on Al surfaces (it must be
pointed out that, the number of free electrons being smaller
in Ag than in Al, very thin Ag films on Al can be regarded,
under certain aspects, as a depletion layer at the Al surface).
We give evidence for the two surface plasmon modes corresponding
to very thin films of Ag on Al, and for the excitation of
surface plasmons at the Al/Ag interface. We show that the
surface plasmon dispersion relation of Al is splitt by a 26 Å
thick Ag layer. This splitting is not observed for thinner
(6 Å) Ag layers. The possibilities of studying in this way the
electronic structure of very thin metallic layers are emphasized.

2.   Experiment

The experimental set-up essentially consists in an ultra-
high vacuum chamber operating in a pressure range of about
10^{-10} torr, equipped with an evaporator with two tungsten
crucibles, a precision goniometer (0.01° angular accuracy)
aligned with an external optical double-beam set-up, which
allows to measure the square of the sample reflection coefficient
R_p^2 (the incident beam is linearly polarized parallel to the
plane of incidence). An Ithaco 353 is used both as a lock-in
amplifier and as an electronic ratiometer. The optical components
are a 250 W tungsten-hologen lamp (0.4-0.9 μm) and a 75 W Xenon
lamp XBO 75 (0.27-0.4 μm).

The samples are Al films, about 200 Å thick, deposited
by vacuum evaporation onto a 60° silica prism. A collimated
p-polarized beam falling on the prism at angles greater than
the critical angle allows to excite SPW at the Al/vacuum surface,
and spectroscopic measurements are carried out by recording
R_p^2 versus wavelength λ for several angles of incidence φ.
Electron microscope investigations show that such Al films have
a good (111) fiber structure, with cristallites of about 2000 Å

in lateral dimensions. The optical constants of the Al films were determined from the ATR curves in the 0.4-0.9 μm spectral range and were found to be in good agreement with the values reported by Mathewson and Myers (12).

Thin films of Ag are then deposited in situ, under the same vacuum, onto the Al surface, the mass of the deposit being monitored by a 5 MHz Sloan oscillating quartz, the calibration of which was previously performed after the determinaton of Al and Ag film thicknesses by X-ray interferometry. The quartz balance sensitivity is 15 Hz for one Å of Ag deposited in this particular arrangement.

The d.c. resistance of the Al film is measured in situ, and its modifications during Ag deposition are recorded simultaneously. Figure 1 shows the variation of the Al film resistance ΔR as a function of the deposited Ag mass (or mass thickness d_f) in the early stages of Ag deposition, in the case which will be discussed optically later on. Since the Al film thickness (d = 214 Å) is of the same order of magnitude as the mean free path of conduction electrons, size effects are expected to be important and the electrical resistance depends on the scattering of the conduction electrons by the film surfaces (13). Adsorption at a surface generally produces an increase of the film resistance (14). It must be noticed first that the Al film resistance increases very fast and linearly versus mass thickness d_f for very small coverages ($d_f < 0.75$ Å). This region probably corresponds to the adsorption of Ag as isolated ad-atoms (14). The levelling off of the curve, followed by a weak minimum located between 3 and 4 Å, reflect a decrease of diffuse scattering, which suggests a more continuous geometry for the deposit. We conclude that, at the beginning (first monolayer), the growth of Ag on an Al (111) surface must be rather continuous. Then, the resistance increases again but smoothly until about $d_f = 15$ Å. For larger thickness, the resistance starts to decrease and it reaches the initial value for the bare Al film ($\Delta R = 0$) for $d_f = 58$ Å. From these results, we deduce that the Ag superficial

layer is then discontinuous. Electron micrographs taken for the largest thickness (d_f = 58 Å) indeed reveal small isolated Ag crystallites of about 200 Å in lateral dimensions, grown in epitaxy with the Al substrate crystallites, and covering about 30% of the Al surface only. Every time we stop the Ag deposition, the resistance does not change during the optical measurements which take about one hour; we thus conclude that metallic diffusion is negligible.

3.   Description of optical results

Figure 2 shows the R_p versus λ curves for an external angle of incidence φ = 37.77°, obtained in ATR experiments performed first on a bare Al film (d = 214 Å), then on the same film covered by Ag layers of increasing thickness: d_f = 2, 6.5, 26, 39 and 58 Å (mass thickness as determined with the oscillating quartz); we shall refer to these layers as 1, 2, 3, 4 and 5 respectively. These curves were corrected for stray light effects at low energies, assuming that the optical constants of Al are, in this spectral range, given by the same Drude formulae which reproduce very well the optical constants in the visible region.

Let us notice that the first layers 1 and 2 give rise to a slight shift and a broadening of the resonance only. This is the general situation observed for the effect of absoring surface layers on the R_p curves (15). The situation is quite different for the following films 3, 4 and 5. There is a strong splitting of the R_p curve, which displays now two resonances instead of a single one. Such an effect was predicted theoretically when the dieelctric constant of the surface layer passes through zero or goes to infinity (16). In fact, as we deal with metals, we also ask that the imaginary part of the complex dielectric constant $\mathcal{E}_f$ be small in order to excite plasma oscillations. In the considered spectral range, Al has a negative dielectric constant and acts indeed as the active medium, but the dielectric constant of Ag takes over negative and then positive values for $\omega > \omega_{pf}$ (the bulk plasma frequency ω_p of Ag is 3.77 eV)

and the SPW condition at the Al/Ag interface can be verified.
We conclude that, at least qualitatively, the Ag surface layers
3, 4 and 5 display a "plasma frequency behaviour" in the explored
spectral range, like bulk Ag.

It is clearly apparent from figure 2 that the spectral
position of the short-wavelength peak is nearly insensitive to
the Ag film thickness, in contradistinction to the long-wavelength
one which is strongly thickness dependent. The short-wavelength
peak is related to SPW excitation at the Al/Ag interface and it
should be observed even for an infinitely thick Ag film (we did
not go further than $d_f = 58$ Å in the present experiments). The
short wavelength peak therefore gives a strong experimental
evidence for SPW excitation at a metal/metal interface. In fact,
due to the small thickness of the Ag layer, both modes are
strongly coupled, and thickness dependent. For thicker films,
it should be possible to look nearly independently at both
surfaces of the Ag film (Ag/vacuum and Ag/Al), simply by
changing the wavelength in a way similar to the method described
for metallic films on dielectric materials (4, 5).

4. Dispersion relation

The SPW dispersion relation can be obtained from the set
of experimental curves similar to those presented in Figure 2,
by taking the spectral position of the R_p minima for each angle
of incidence (the experiments are indeed carried out at fixed
angle of incidence by varying the wavelength). Figure 3 shows
the dipsersion curves ω versus the reduced wavevector $s = k/k_o$,
where k is the wavevector parallel to the surface and $k_o = \omega/c$,
in the case of surface layers 3, 4 and 5 where a splitting is
observed. The situation is quite different if we fix the wave-
length and draw the R_p curves as a function of wavevector.
Figure 4 shows the dispersion curve obtained in this way for
surface layer 3 ($d_f = 26$ Å) (curve with stars). The striking

difference between these two types of dispersion relation must be emphasized: the dispersion curve obtained from experimental ATR data at fixed wavelength is a continuous line (figure 4) while the dispersion curve obtained from data at fixed angle of incidence presents a discontinuity and consists in two distinct branches (figure 3). As explained before (7), this phenomenon is related to damping effects.

The SPW dispersion relation for a metallic layer ($\mathcal{E}_f$, d_f) on a metallic substrate ($\mathcal{E}_o$) is given by the implicit equation (17, 18):

$$Z + Z_c + (Z Z_0 / Z_f + Z_f) \tanh \theta = 0 \qquad (1)$$

which gives the poles of the reflection coefficient for this layered system. Z is the optical admittance defined in each case by $Z = \mathcal{E} (\mathcal{E} - s^2)^{-1/2}$ and θ is given by $\theta = k_o d_f (s^2 - \mathcal{E}_f)^{\frac{1}{2}}$. The indices o and f refer to the substrate (Al in our case) and the surface layer of thickness d_f (Ag our case) respectively: k, k_o and s have been defined earlier. Equation (1) must be solved with complex values of $\omega = \omega_1 - i \omega_2$ if one deals with experiments performed at variable frequency (fixed angle of incidence), but with complex values of the reduced wavevector $s = s_1 + i s_2$ if one deals with experiments performed at variable angle of incidence (fixed frequency).

The continuous line in figure 4 represents the dispersion relation $\omega(s_1)$ obtained by solving equation (1) with s complex in the case of layer 3 (d_f = 26 Å). For the Al substrate, we have taken a dielectric constant $\mathcal{E}_c$ given by the Drude expression:

$$\mathcal{E}_c = 1 - \omega_p^2 / \omega^2 [1 + i (\omega \tau)^{-1}],$$

with ω_p = 14,88 eV and $\omega_p \tau$ = 24,85, which gives excellent agreement with our experimental results for bare Al. The parameters are identical to those reported by Hunter (19). For the Ag surface layer, we have tried for $\mathcal{E}_f$ the values given by Dujardin and Thèye (20), which have been introduced numerically in order to solve equation (1). In figure 3, we have represented in the same way the dispersion relation $\omega_1(s)$ obtained by solving equation (1) with ω complex, in the case of layers

3, 4 and 5 (d_f = 26, 39 and 58 Å). Here we need an analytical expression to describe the behaviour of the Ag dielectric constant with frequency, $\varepsilon_f(\omega)$. In the region of interest, i.e. in the vicinity of its plasma frequency ω_p = 3.77 eV, the Ag dielectric constant cannot be represented by a free electron model only (like the Al one), because the contribution of interband transitions, which give a steep absorption edge at energies greater than the onset at 3.86 eV (20), cannot be neglected. A realistic representation of the dielectric constant in this spectral range is a rather difficult problem (21) and we have tried the expression:

$$\varepsilon_{f.1} = P - (\omega_{pf}/\omega)^2 + a \, Real(\underline{r})$$
$$\varepsilon_{f.2} = \omega_{pf}^2/\omega^3 \tau_f + b \, Im(\underline{r})$$

(2)

with

$$\underline{r} = \left[(\omega_g + \omega + i\Gamma)^{1/2} - (\omega_g - \omega - i\Gamma)^{1/2}\right]/\omega.$$

The first term in each expression accounts for intraband transitions of conduction electrons. The second term intends to describe the contribution of interband transitions near the absorption edge. It must be noticed that a contribution proportional to $\underline{r}$ is obtained if one assigns an oscillator with constant oscillator strength to every transition between two parabolic bands. As far as our problem here is concerned, the important point is that equations (2) reproduce within experimental uncertainties the Ag dielectric constant in the spectral region where SPW can propagate. Moreover, we have verified that the chosen analytical expression does not influence apprecibly the results concerning the SPW dispersion relations. The values of ω_{pf} and τ_f are taken from (20) and a simultaneous least squares fit of the real and imaginary parts of the Ag dielectric constant given in (20) leads to the remaining parameters of the model. The values used in the end are then:

ω_{pf} = 9.98 eV, ω_{pf}^2/τ_f = 3.37(eV)^3, ω_g^2 = 3.99 eV, Γ = 0.035 P = -7.93, a = 23 eV$^{-1/2}$ and b = 35.9 eV$^{-1/2}$.

The large negative value of P balances the positive contribution from the real part of $\underline{r}$, which is certainly overestimated.

Before discussing the curves in figures 3 and 4, it must be emphasized that all our treatments of the data assume first

that the surface layer is a continuous homogeneous layer with
plane parallel surfaces, having the same dielectric constant
as bulk Ag, second that one has a local dielectric constant $\varepsilon(\omega)$.
We shall come back later to the first basic hypothesis. As for
the second one, if it seems to be a good approach for thick
enough films, i.e. for films 3, 4 and 5, this is probably not
the case for very thin films like films 1 and 2, because the
component of the electric field perpendicular to the surface
varies very quickly over distances comparable to the surface
layer thickness. We have also neglected spatial dispersion effects
coming from the longitudinal wave which can propagate in Ag for
frequencies greater than ω_{pf} (22, 23, 24). We are dealing here
with a geometry which should be particularly sensitive to such
effects, the wavelength of longitudinal waves being about two
orders of magnitude shorter than the wavelength of transverse
waves, and size effects being therefore expected for films with
thicknesses of the order of the present ones, provided they are
continuous. Unfortunately, Ag in the region of interest does
not present a simple free-electron like behaviour and the theory
in this case has still to be done.

Going back to figure 3, we see that for layer 3 (d_f = 26 Å)
the experimental points (obtained from experiments at fixed
angle of incidence) are in good agreement with the computed
curve, at least for the high energy branch; for the low energy
branch, the experimental points are shifted towards larger values
of s. For layers 4 and 5 (d_f = 39 and 58 Å), the discrepancy
between experimental and computed values increases, especially
for the low energy branch. The upper branches have been drawn
starting from s = 1 only, but in fact they start already at
s = 0. Damping mixes the Brewster mode and the Fano mode and the
two surface electromagnetic excitations are no more separated
(25). On the other hand, the upper branches must stop at s = 1.06,
1.062 and 1.075 for layers 3, 4 and 5 respectively, as shown
in figure 3. This is again an effect of increasing damping in
the layer. As it clearly appears in figure 3, the experimental
branches do not stop at the computed values. We have verified,

both on experimental $R_p(\lambda)$ curves and on computed ones, that the
minimum at low wavelength disappears indeed at larger angles of
incidence. In order to understand this discrepancy, several
reasons can be put forward: a) experimental errors arising from
the fact that the minimum of the $R_p(\lambda)$ curves becomes flatter
and flatter; b) optical constants of the Ag surface layer slightly
different from the bulk optical constants which we have used
in the computations; c) omission, in the calculation of the
dispersion relations, of the finite thickness of the Al substrate
film and of the presence of the prism.

The arrows in figure 3 indicate the frequencies at which
the reflectivity measured on the same systems from the external
side (vacuum side) presents a minimum. This minimum shifts to
smaller energies and its intensity increases with increasing d_f:
$\omega_m \simeq 3.78$ eV for layer 3, 3.76 eV for layers 4 and 5. Its
position is the same for different angles of incidence: 30, 40
and 60°. It must be associated to the plasma frequency of the
Ag surface layer. We see that the splitting of the dispersion
curves occurs, as expected, around the frequencies indicated
by the arrows. The shift to smaller frequencies is, at least
qualitatively, consistent with the fact that the experimental
points move away, in the same direction, from the computed curves
when d_f increases.

It is difficult to discuss the discrepancy which exists
between experimental and computed dispersion relations. It is
probably essentially due to the discontinuous character of the
Ag surface layer, as described earlier from electron microscope
studies. A granular layer will produce scattered light into
vacuum, leading to a shift and a broadening of the resonance
(26, 27). The shift is towards larger angles of incidence,
therefore in the same direction as the effects noticed in our
results. Moreover, but this may be a secondary effect, the
assumption that the dielectric constant of the surface layer is
equal to the bulk Ag dielectric constant must break down for
small grains, especially for the conduction electron contribution,

since their relaxation time must be sensitive to the grain size.

In all the former discussions, we have completely neglected the case of the thinner surface layers 1 and 2, for which no splitting of the minimum in the $R_p(\lambda)$ curves is observed. It is remarkable to see that the reflectivity measured from the vacuum side does not either present a minimum in these two cases, at least in the explored spectral range. We suggest that, for so small coverages (d_f = 2 and 6.5 Å), the Ag clusters or micro-crystallites are not large enough to have a well-defined plasma frequency, or that the plasma resonance is damped by collision effects. The effects discussed in the present paper, related to the fact that the dielectric constant of the metallic surface layer passes through zero in the spectral range where the active medium is examined, are not present. These films must then be treated in the same manner as in the general case of an absorbing surface layer on a metal surface (15). However, any interpretation of this kind is highly speculative as long as non-local effects and spatial dispersion are neglected.

A final point which must be made is to emphasize the sensitivity of the method based on the effects described here to detect very thin metallic surface layers on a metal surface, if these layers present the expected bulk dielectric constant. The splitting observed in the reflectivity curves is indeed very important, even for quite thin films. For a free electron gas behaviour (with λ_{pf} the plasmawavelength of the film larger than λ_{po} the plasmawavelength of the Al substrate, like in our case), the wavelength splitting $\delta\lambda$ is given (7, 18) by:

$$\delta\lambda/\lambda_{pf} \simeq \pm \left(\pi d_f/\lambda_{po}\right)^{1/2}. \tag{3}$$

The fact that $\delta\lambda$ is proportional to $\left(d_f/\lambda_{po}\right)^{1/2}$ and not to d_f/λ_{po}, as it is generally the case for the optical response to very thin films ($d_f/\lambda \ll 1$), leads to an increase of sensitivity for very small values of d_f/λ. For example, the splitting observed for layer 3 (d_f = 26 Å) is 800 Å, i.e. about 30 Å per Å. On the other hand, it is quite easy to determine, at least qualitatively,

at what thickness the surface layer reaches a behaviour close
to the expected bulk one, just by looking at the rough experi-
mental data, without any other sophisticated analysis.

5.   Conclusion

We have performed ATR experiments on Ag surface layers of
increasing thicknesses (from 2 to 58 Å) deposited on an Al surface
in a spectral range (0.27 - 0.9 μm) in which Al is highly
reflecting (active medium) and the dielectric constant of Ag
passes through zero at the plasma frequency. We have shown that,
for not very thin surface layers ($d_f \geqslant 26$ Å), the predictions
of the theory are roughly verified, even if the surface layers
are largely discontinuous. We have indeed observed a splitting
of the SPW dispersion relation around the surface layer plasma
frequency, and we have given experimental evidence for SPW
excitation at the metal/metal (Al/Ag) interface. We have
discussed why no splitting is observed for the thinnest surface
layers. We have eventually emphasized the sensitivity of such a
method for the detection of thin metallic layers on a metal
surface.

References

1. RITCHIE R.H., _Phys. Rev._ 106 (1957) 874.

2. FERREL R.A., _Phys. Rev._ 111 (1958) 1214.

3. BRILLSON L.J., _Phys. Rev. Lett._ 38 (1977) 245.

4. ABELES F. and LOPEZ-RIOS T., _Opt. Commun._ 11 (1974) 89.

5. KOVACS G.J. and SCOTT G.D., _Phys. Rev._ B 16 (1977) 1297.

6. STERN E.A. and FERREL R.A., _Phys. Rev._ 120 (1960) 130.

7. LOPEZ-RIOS T., _Opt. Commun._ 17 (1976) 342.

8. GUIDOTTI D. and RICE S.A., _Phys. Rev._ B 14 (1976) 5518.

9. CONWELL E.M., _Phys. Rev._ B 14 (1976) 5515.

10. GUIDOTTI D. and RICE S.A., _Solid State Commun._ 15 (1974) 113.

11. GUIDOTTI D. and RICE S.A., _Chem. Phys. Lett._ 46 (1977) 245.

12. MATHEWSON A.G. and MYERS H.P., _Phys. Scripta_ 4 (1971) 291.

13. FUCHS K., _Proc. Camb. Phyl. Soc._ 34 (1938) 100.

14. PARISET C. and CHAUVINEAU J.P., _Surf. Sci._ 47 (1975) 543.

15. ABELES F. and LOPEZ-RIOS T., _Proc. 1st Taormina Res. Conf. on Structure of Matter: Polaritons_ (edited by BURSTEIN E. and DE MARTINI F., Pergamon Press, New York) 1974 , p. 241.

16. AGRANOVICH V.M. and MALSHUKOV A.G., _Opt. Commun._ 11 (1974) 169

17. ECONOMOU E.N. and NGAI K.L., _Adv. in Chem. Phys._ (edited by PRIGOGINE I. and RICE S.A.)vol.27 1974 , p. 298.

18. ABELES F., _Thin Solid Films_ 34 (1976) 291.

19. HUNTER W.R., _J. Physique_ 25 (1964) 154.

20. DUJARDIN M.M. and THEYE M.L., _J. Phys. Chem. Solids_ 32 (1971) 2033.

21. GUERRISI M., ROSEI R. and WINSEMINS P., _Phys. Rev._ 12 (1975) 557.

22. FORSTMANN F., *Z. Phys.* 203 (1967) 495.

23. MELNYK A.R. and HARRISON M.J., *Phys. Rev.* B 2 (1970) 835.

24. JONES W.E., KLIEWER K.L. and FUCHS R., *Phys. Rev.* 178 (1969) 1201.

25. OTTO A., *Optical Properties of Solids, New Developments* (edited by SERAPHIN B.O., North Holland Publishing Co., Amsterdam) 1976. p. 678.

26. HORNAUER D., KAPITZA H. and RAETHER H., *J. Phys.* D 7 (1974) L-100.

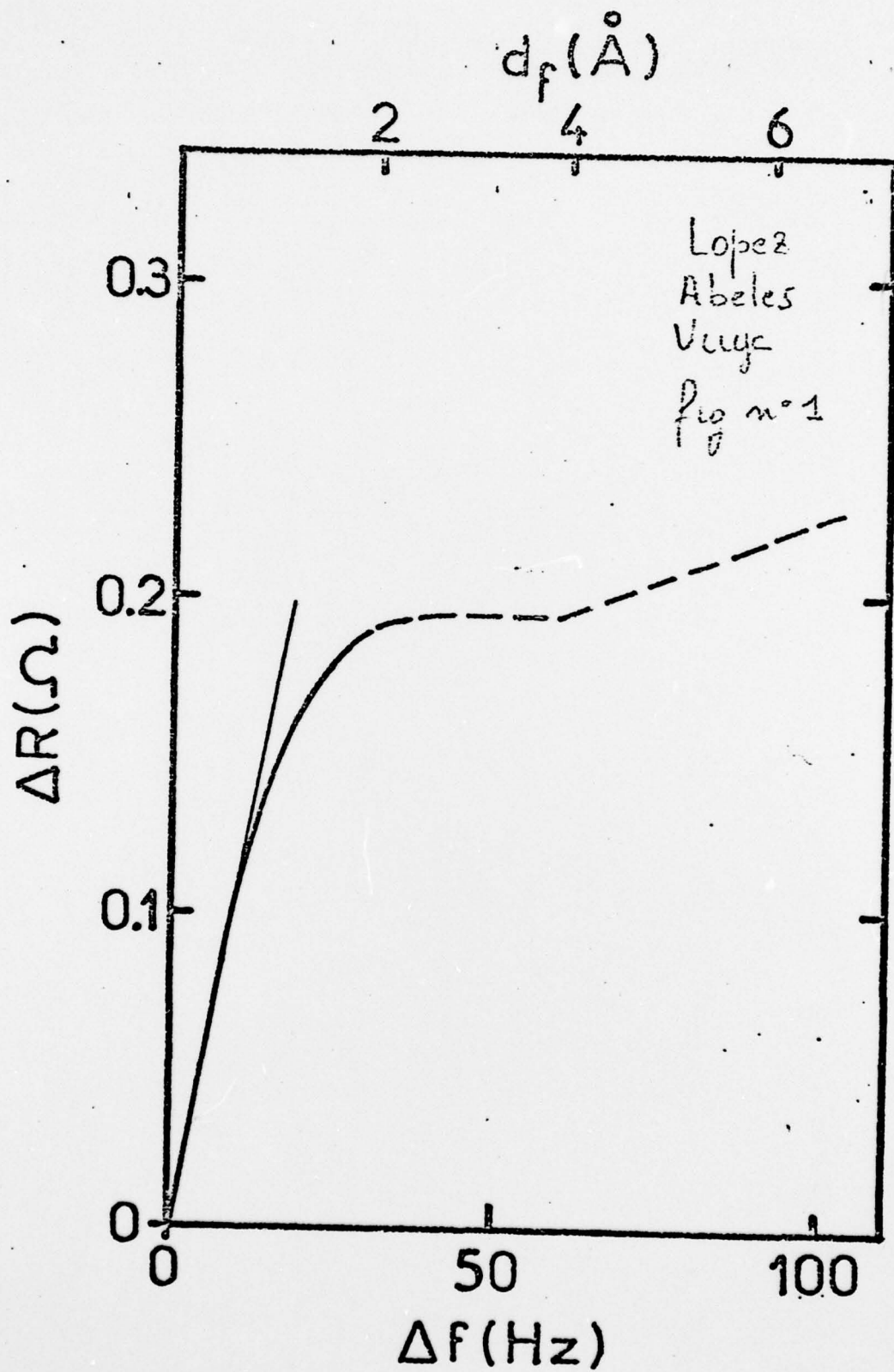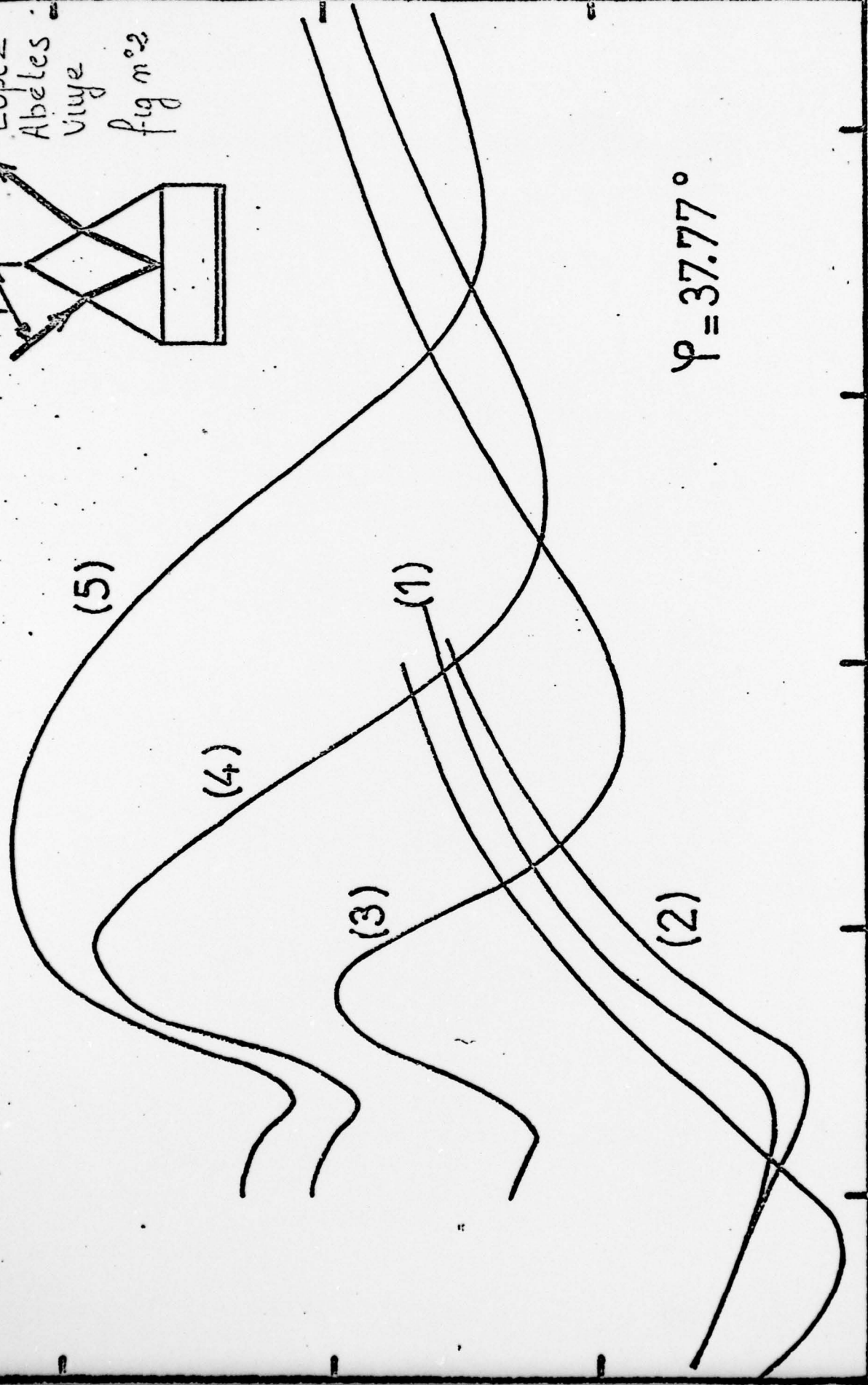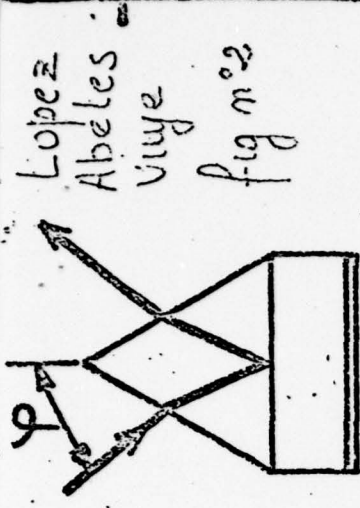27. POCKRAND, *J. Phys. Lett.* 49A (1974) 259.

Figure captions

Figure 1 : Modification of the resistance ΔR of an Al thin film 214 Å thick with initial resistance $R_o = 3\Omega$, during the deposition of Ag films 1 (continuous line) and 2 (discontinuous line).

Figure 2 : Reflection coefficient R_p as a function of wavelength for an ATR experiment with an Al thin film 214 Å thick deposited on a 60° silica prism and covered by Ag layers 2, 6,5, 26, 39 and 58 Å thick labelled by numbers 1, 2, 3, 4 and 5. The external angle of incidence was 37.77°.

Figure 3 : ω_1 versus s as computed with equation (1) for complex values of the frequency $\omega = \omega_1 - i\omega_2$ for Ag layers of thickness 26 Å (continuous line), 39 Å (dotted and dashed line) and 58 Å (dashed line); the corresponding experimental values are also indicated: full circles for layer 3, open circles for layer 4 and crosses for layer 5.
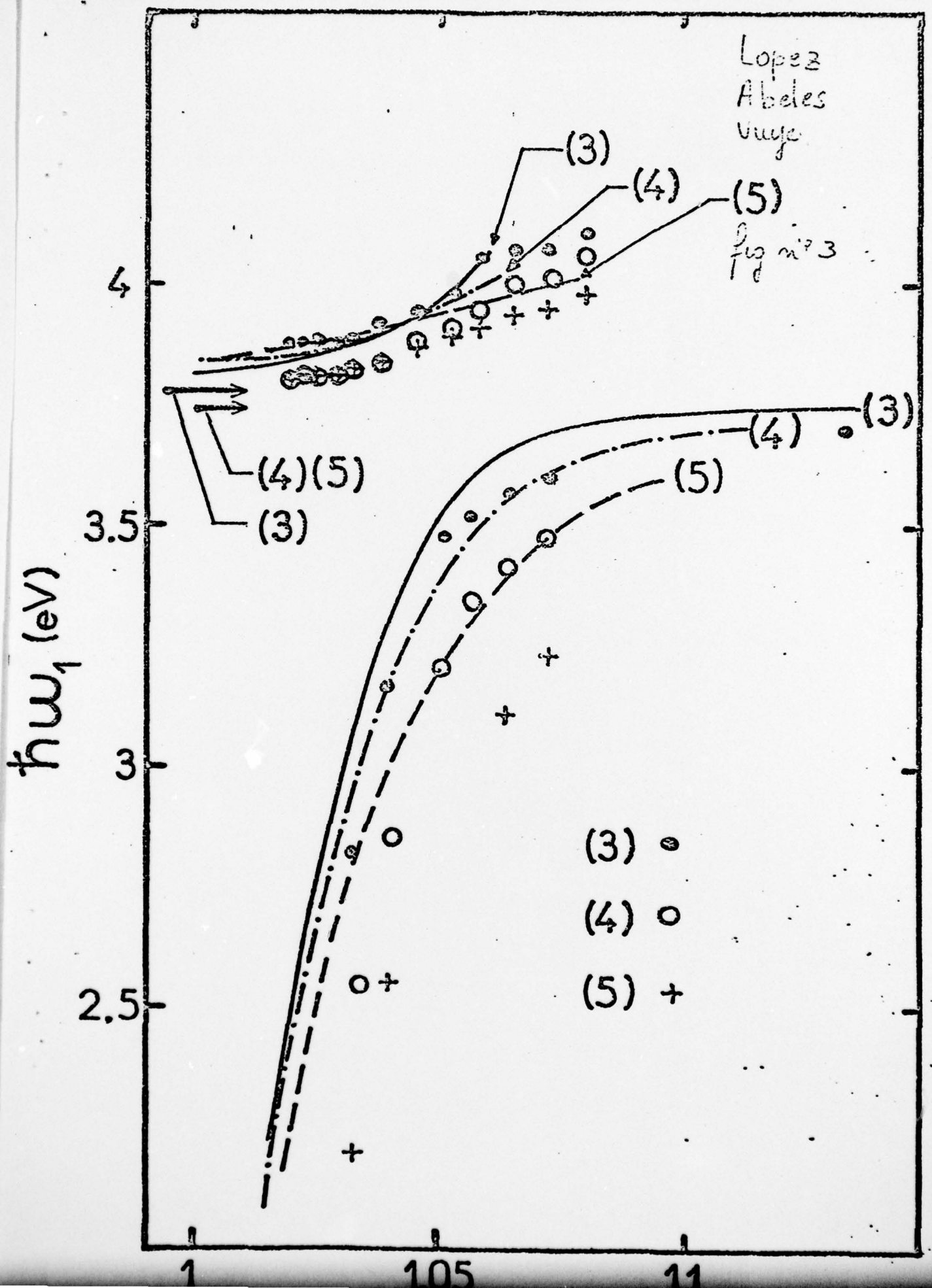
Figure 4 : ω vs s_1 computed with equation 1 for complex values of $s = s_1 + is_2$ for an Ag layer 26 Å thick (continuous line), the experimental points are represented by crosses.
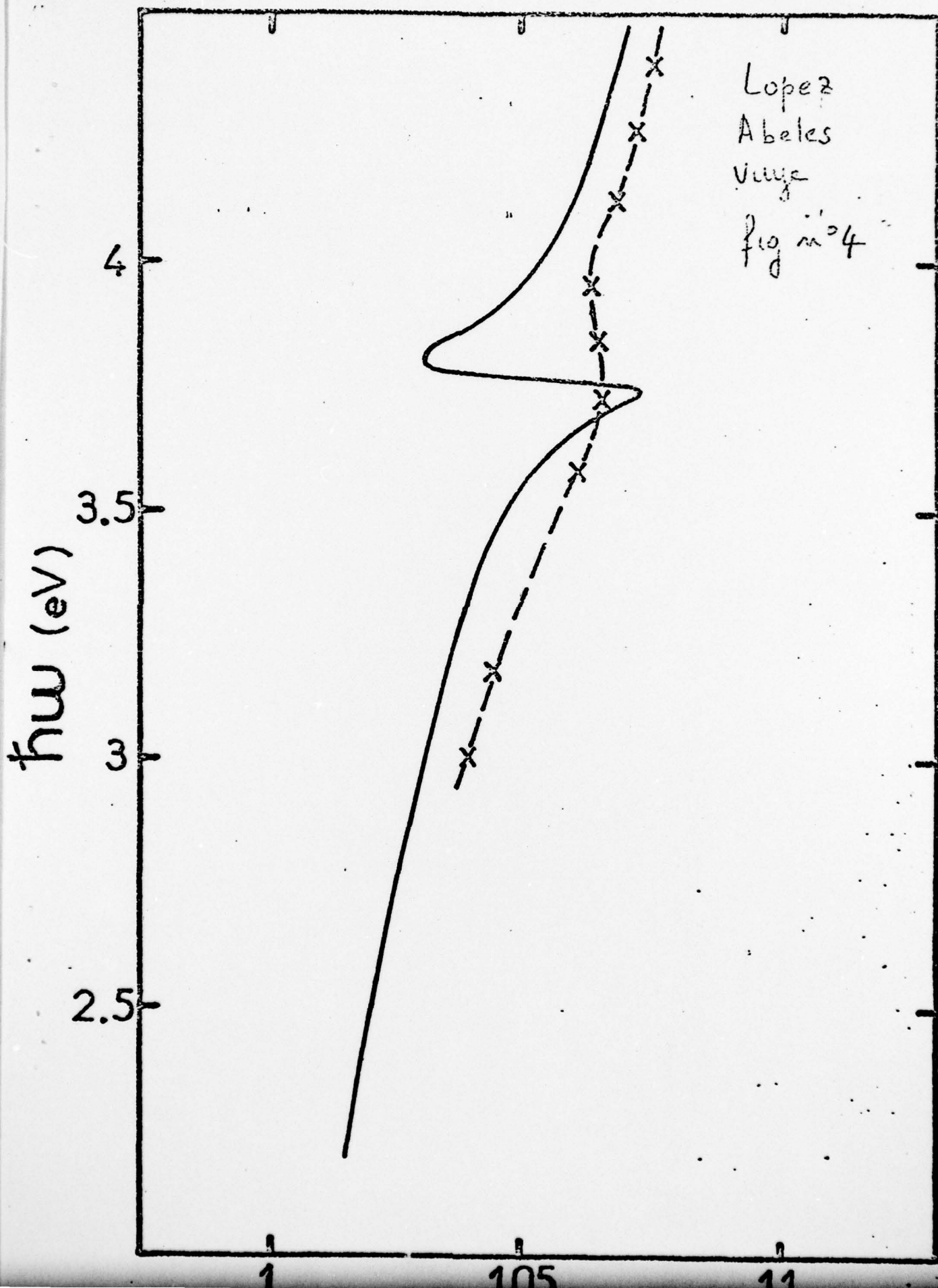
Lopez
Abeles
Vuye

fig n°1

Lopez
Abeles
Viuye
fig n°2

$\varphi = 37.77°$

(1) (2) (3) (4) (5)

$\lambda(\text{Å})$

3000   4000   5000

Lopez
Abeles
Vuye

fig nº 3

Lopez
Abeles
Vuye

fig n°4

APPENDIX VI

INVESTIGATION OF THE METAL–ELECTROLYTE INTERFACE USING SURFACE PLASMA WAVES WITH ELLIPSOMETRIC DETECTION

F. Abelès and T. Lopez-Rios[*]

Laboratoire d'Optique des Solides,[†] Université Paris VI, 4 Place Jussieu, 75230 Paris, Cedex 05, France

and

A. Tadjeddine

Laboratoire d'Electrolyte du CNRS, 1 Plance A. Briand, 92190 Meudon, France

Use of ellipsometric detection of surface plasma waves at the metal–electrolyte interface enables a decoupling of the effects of an applied voltage on the electrons of the metal and on the ions of the electrolyte. Experimental results for the Au–H_2SO_4 and $HClO_4$ interfaces are presented. It is found that the penetration depth of the applied voltage in the metal, for not too large modifications of the surface charge (up to 2.5×10^{14} electrons/cm^2), is $1–1.5$ times the Thomas–Fermi screening length.

THE INVESTIGATION of the metal–electrolyte in interface is a subject of current interest, the aim being a better understanding of electrochemical reactions and electro–catalysis process as well as polarization effects in the ionic double layer region.[1,2] Here very strong electric fields can exist, which perturb the neighbourbood of the interface. Their penetration depth in the metal is extremely short and is given by the Thomas–Fermi length, l_{TF}, which is less than 1 Å, indication that the static field due to a test charge at the surface of a metal is screened out within the first atomic layer. Electro-reflectance experiments by modulation of the applied voltage at the interface have been performed successfully,[3] but their interpretation is still somewhat obscure.[4]

This communication demonstrates theoretically and experimentally that by using surface plasma (SP) waves propagating along the metal–electrolyte interface, it is possible to obtain unambiguous information on the effect of the applied electric field on both media. The technique employed is the optical excitation of SP by attenuated total reflection (ATR) and their ellipsometric detection.[5]

SP are collective oscillations of the free charges at the metal surface, which can be excited optically by a p-polarized wave only. The excitation of SP waves is conspicuous through a resonance minimum of the reflected (complex) amplitude, which occurs when the component of the wave-vector along the surface, $K = K_1 + iK_2$, reaches the value $K_m^2 = (\omega/c)^2 \epsilon\epsilon_s / (\epsilon + \epsilon_s)$, ϵ and ϵ_s being the dielectric functions of the media in contact. The advantage of ellipsometry is to give information on both amplitude and phase of the p-reflected component of the electric field vector.

Surface plasma waves propagate along the ϵ/ϵ_s interface and their amplitude is exponentially decaying on both sides of it. They are, therefore, sensitive to any modification occuring at that interface. The

* Recipient of a scholarship "Formacion del personal investigador" of the Spanish Government.
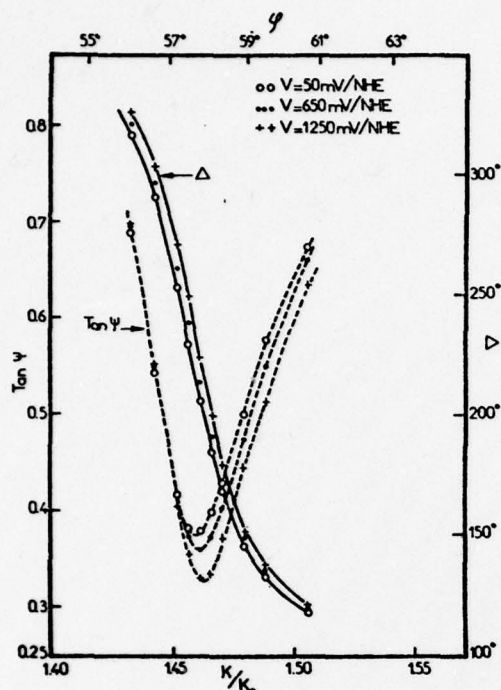
† Equipe de Recherche Associée au C.N.R.S.

FIG. 1. Tan Ψ and Δ vs K/K_0 for an Au-film (thickness = 408 Å) in a $1NH_2SO_4$ solution, $\lambda = 6093$ Å, for three different applied voltages. The displacement of the minimum (resonance) of tan Ψ is given by $\Delta K_1/K_0$. The upper scale for the abscissas indicates the angles of of incidence at the prism–Au-film interface.

experiments to be described make use of this sensitivity. Essentially, any modification which is localized in the immediate vicinity of the interface will add a wave-vector $\Delta K = \Delta K_1 + i\Delta K_2$ to K. The experiments which are reported here enabled the measurement of ΔK as a function of the applied voltage, which provided information about the very thin perturbed region close to the interface. Application of a static electric field at the metal–electrolyte interface affects both media. In the metal, electronic effects are predicted, which, although limited to an extremely thin region (thickness $l_{TF} \lesssim 1$ Å), can be extremely strong, d.c. electric fields of the order of 10^7 V/cm being easily attained. The surface of the transparent electrolyte is also perturbed with the formation of an ionic double layer showing or not specific anion adsorption. The ionic double layer is subjected to large electrostrictive compression, which should increase its dielectric constant. Therefore the measured ΔK must contain contributions from both modifications It can be shown
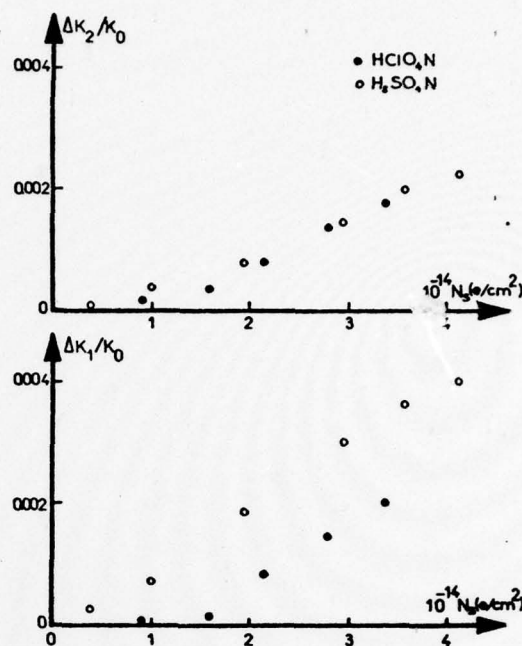

FIG. 2. $\Delta K_1/K_0$ and $\Delta K_2/K_0$ vs displaced surface electric charge N_s in electrons/cm^2 for $1NH_2SO_4$ solution (circles) and $1NHClO_4$ solution (solid circles). The wavelength is $\lambda = 6093$ Å.

that, for layer thickness much smaller than the wavelength, these contributions, ΔK_{metal} and $\Delta K_{electrolyte}$, are additive:

$$\Delta K = \Delta K_{metal} + \Delta K_{electrolyte} .$$

Moreover, the imaginary part of each ΔK is proportional to the imaginary part of the dielectric function of the corresponding very thin layer. The dielectric function of the electrolyte being real (the electrolyte is non-absorbing), $\Delta K_2 = K_{2\,metal}$. It is thus possible to separate the contributions due to electronic effects in the metal and to ionic effects in the electrolyte.

The experimental arrangement consists in an electrochemical part, which has already been described [6] and an ellipsometer with phase and amplitude modulation.[7] The electrochemical cell has been designed in order to allow ellipsometric measurements with SP excitation by ATR. The electrode is a thin gold film vacuum-evaporated on a prism of high index of refraction. The counter-electrode is an Au grid of large reactive surface and the reference electrode is a Hg_2SO_4 electrode. The solution is kept free from oxygen by a

permanent flow of pure nitrogen. The solutions are prepared from Merk Suprapur products and quadri-distilled water (resistivity larger than 18 MΩ·cm). The electrode is cleaned and activated in the cell by a series of cycles of oxydation and reduction before each experiment. The I vs V curves, giving the intensity of the current as a function of the applied voltage, are recorded during the experiment in order to enable a control of the reproducibility.

Ellipsometric measurements give the angles Ψ and Δ which are related to the complex reflected amplitudes r_p and r_s for electric field parallel and perpendicular to the plane of incidence through $\tan \Psi \exp (i\Delta) = r_p/r_s$. The amplitudes of the incident fields are taken as unity. The measurements were performed as a function of the angle of incidence ϕ at the prism–gold film interface at fixed wavelength $\lambda = 6093$ Å ($\hbar\omega = 2.034$ eV) for different values of the potential of the Au electrode (film) between 50 and 1250 mV (NHE). The results are shown on Fig. 1 in the vicinity of the SP resonance ($56° < \phi < 61°$).

It has been shown[5] that, for a metal film of finite thickness, we can write in this region:

$$\tan \Psi \, e^{i\Delta} \simeq e^{i\Delta_m} \frac{K - (K_m + \Delta K) - \Delta K_f}{K - (K_m + \Delta K) - \Delta K_f} \quad (1)$$

where $K = K_0 \cdot n_0 \sin \phi$ is the component of the incident wave-vector along the Au-film surface, $n_0 = 1.728$ is the refractive index of the prism and $K_0 = (\omega/c)\cdot$ $\Delta K_f = \Delta K_{f1} - i\Delta K_{f2}$ accounts for the damping of the wave due to the finite thickness d of the Au film (independent measurements gave $\epsilon = -10.9 - i \times 1.42$, $d = 408$ Å for the Au-film used in the experiment leading to the curves of Fig. 1).

The shape of the $\tan \Psi$ vs K curve is apparent from equation (1):

$$\tan^2 \Psi = \frac{(K - K_{m1} - \Delta K_1 - \Delta K_{f1})^2 + (K_{m2} + \Delta K_2 - \Delta K_{f2})^2}{(K - K_{m1} - \Delta K_1 - \Delta K_{f1})^2 + (K_{m2} + \Delta K_2 + \Delta K_{f2})^2}. \quad (2)$$

This shows that the position of the resonance, that is to say of the minimum of $\tan \Psi$, corresponds to $K = K_{m1} + \Delta K_{f1} + \Delta K_1$. Any modification of the metal–electrolyte interface leads to a shift of the position of the minimum of $\tan \Psi$, due to the ΔK_1 term. Simultaneously, the intensity of the resonance is modified by the $K_{m2}/\Delta K_{f2}$ ratio: it can either increase or

decrease with increasing values of ΔK_2. In our case, the Au film being rather thin, $K_{f2} > K_{m2}$ and the minimum value of $\tan \Psi$ decreases with increasing ΔK_2.

Let us assume that the Au-electrolyte (ϵ/ϵ_s) interface contains a very thin layer of thickness d_a and dielectric constant $\epsilon_a = \epsilon_{a1} - i\epsilon_{a2}$. It can be shown[5] that, for this situation

$$\Delta K_a = \Delta K_{a1} - i\Delta K_{a2} =$$
$$\frac{(-\epsilon\epsilon_s)^{1/2}}{-\epsilon + \epsilon_s} K_m^2 \left[1 - \left(\frac{K_m}{K_0}\right)^2 \left(\frac{1}{\epsilon_a} + \frac{\epsilon_a}{\epsilon\epsilon_s}\right)\right] d_a . \quad (3)$$

This is a first order approximation only, but it is quite sufficient for very thin surface layers, when $K_0 d_a \ll 1$. If there are two superimposed very thin surface layers (ϵ_a, d_a) and (ϵ_b, d_b), then, in the same approximation: $\Delta K = \Delta K_a + \Delta K_b$, where ΔK_b is the expression obtained from ΔK_a by replacing ϵ_a, d_a by ϵ_b, d_b. Another point to be noticed is the fact that for $\epsilon_2 \ll |\epsilon_1|$, which is pratically our case, we have ΔK_{a2} and ΔK_{b2} respectively proportional to ϵ_{a2} and ϵ_{b2}.

We are now in a position to discuss our experimental results which are summarized by the ΔK_1 vs N_s and ΔK_2 vs N_s curves of Fig. 2, where N_s is the total excess electronic surface charge per unit area required to shield the field (estimated for each value of the applied voltage). The zero charge potential of the Au–acid system being poorly known, we have determined the values of the charges for the various voltages used by taking $q = 0$ for $V = 50$ mV. The charges have been computed from the curves giving the differential capacity vs voltage for systems similar to ours[8] and found to be in good agreement with our I vs V experimental curves. Open circles give the results obtained with a $1NH_2SO_4$ solution and solid circles refer to a $1NHClO_4$ solution used as electrolyte.

The striking features of these curves are:

(a) ΔK_2 vs N_s are the same for both electrolytes;

(b) ΔK_1 is approximately proportional to N_s in both cases, the K_1 vs N_s curves being shifted and parallel for $N_s > 1.5 \times 10^4$ el/cm^2.

These results can be interpreted by using a model in which both the electrolyte and the metal electrode are altered by the applied voltage. These modifications give rise to small components of the wave-vector along the surface: ΔK_a for the metal and ΔK_b for the electrolyte. The contribution of the electrolyte to the measured ΔK_2 being zero (the electrolyte is transparent and ΔK_b real), the fact that for a same value of N_s, ΔK_2 has the same value, irrespective of the electrolyte, indicates that the electronic structure of the metal at the interface is modified in the same way. This is consistent with the McIntyre–Aspness model,[9] which assumes, to a first approximation, that interband transitions are unaffected by the applied voltage (which is reasonable in our case because $\hbar\omega$ is smaller than the interband absorption onset) and only the plasma frequency of the free-electron gas in the surface region (thickness $d_a \simeq l_{TF}$) is shifted by an amount proportional to N_s/d_a. As a test of this model, we have computed the d_a values resulting from the experimental ΔK_2. For $N_s \leqslant 2.5 \times 10^{14}$ electrons/cm^2, the d_a values were found to vary from 0.6–0.9 Å, that is to say from l_{TF} to 1.5 l_{TF}. For larger values of N_s, it was impossible to find a value for d_a which would reproduce the measured ΔK_2. This is not surprising because, for such high values of N_s, the simple McIntyre–Aspness model is not expected to be valid any more.

The ΔK_1 values computed with the McIntyre–Aspnes model (ΔK_{a1} in our notation) are much smaller than the experimental values, over the whole range of N_s for the H$_2$SO$_4$ electrolyte, and for $N_s > 1.5 \times 10^{14}$ electrons/cm^2 for the HClO$_4$ electrolyte. The experimental ΔK_1 must thus essentially be related to modifications of the electrolyte in the vicinity of the surface: $\Delta K_1 \simeq \Delta K_{b1}$. The ΔK_1 vs N_s variations are easily understood in a model already suggested by Paik et al.[10] in which the dielectric function ϵ_b is a function of the relative-coverage θ of the metallic surface by ions, the

thickness d_b of the sub-monolayer region being taken as a constant. According to its definition, $\theta = q_-/q_{sat}$, q_- being the amount of adsorbed ions and q_{sat} the value of q_- at full coverage. If we correlate ϵ_b to the amount of adsorption according to reference 10, it can be shown that $\epsilon_b = \epsilon_s + [B/d_b - (\epsilon_s - 1)/(\epsilon_s + 2)]$, B being a constant characteristic of the adsorbate. Equation (3), with ϵ_b, d_b replacing ϵ_a, d_a leads to $\Delta K_{b1}/K_m = $ const. $[B - (\epsilon_s - 1)d_b/(\epsilon_s + 2)]\theta$. If it is assumed that $q_- = N_s - N_{s_0}$, N_{s_0} being the charge corresponding to the voltage at which specific adsorption starts, and if one notices that q_{sat} is the same for SO$_4^{2-}$ and ClO$_4^-$ according to reference 10, the above relation between ΔK_{b1} and θ is consistent with the experimental ΔK_1 vs N_s variations. Thus our experimental results indicate that, for ClO$_4^-$, specific adsorption starts for $N_{s_0} = 1.5 \times 10^{14}$ electrons/cm^2, i.e. 650 mV/NHE, in agreement with the results of Schmid and Hackerman,[11] whereas for SO$_4^{2-}$ it starts at a much lower voltage, which is also generally admitted. The fact that the K_1 vs N_s curves run parallel for the two electrolytes is an indication of the fact that the quantity $B - [(\epsilon_s - 1)d_b/(\epsilon_s + 2)]$ is very close for both.

In conclusion, we have demonstrated that by using ellipsometry with SP it is possible to investigate the effect of the electric field at the metal–electrolyte interface and to decouple the electronic effects in the metal from the ionic effects in the electrolyte. Although the method can be used with a free-electron-metal only, its sensitivity is high and the interpretation of the experimental results is straightforward. We are investigating now the region of oxygen adsorption in the same Au–electrolyte systems.

REFERENCES

1.   MCINTYRE J.D.E., *Advances in Electrochemistry and Electrochemical Engineering*, Vol. 9, John Wiley (1973).

2.   BOCKRIS J.D'M and REDDY A.K.N., *Modern Electrochemistry*, Plenum, New York (1970).

3.   FEIBLEIB J., *Phys. Rev. Lett.* 16, 200 (1966).

4.   GARRIGOS R., KOFMAN R. and RICHARD J., *Solid State Commun.* 14, 1029 (1974).

5. ABELES F. and LOPEZ-RIOS T., *Proc. Taormina Conf. on Structure of Matter "Polaritons"*, (Edited by BURSTEIN E.) p. 241, Pergamon, New York (1974).

6. CHAO F., COSTA M. and TADJEDDINE A., *Bul. Soc. Chim. France 7*, 2465 (1971).

7. WILMANNS J., *Surf. Sci.* **16**, 147 (1969).

8. SOTTO M. (private communication); VENNERAN P., (to be published).

9. MCINTYRE J.D.E. and PECK W.S., *Far. Disc. Chem. Soc.* **56**, 122 (1973).

10. PAIK W., GENSHAW M.A. and BOCKRIS J.O'M., *J. Phys. Chem.* **74**, 4266 (1970).

11. SCHMID G.M. and HACKERMAN N., *J. Electroch. Soc.* **109**, (3), 243 (1962).